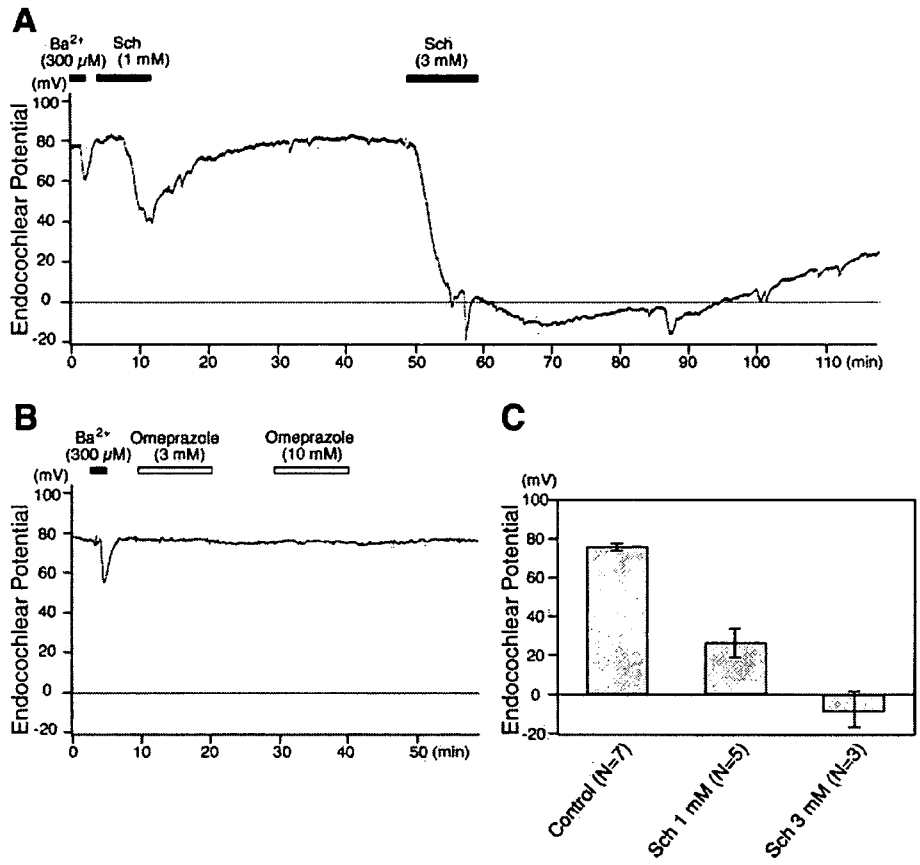

Fig. 6. Effects of vascular perfusion of blockers of gastric H^+,K^+-ATPase on EP. The EP of guinea pigs was measured with vascular (*A* and *B*) perfusion of the blockers Sch-28080 and omeprazole. The blockers were applied for the periods indicated by horizontal bars, as described in MATERIALS AND METHODS. *C*: effects of Sch-28080 on EP under different conditions. Error bars represent SE.

of ~100–300 μM. Because it was also shown in many previous studies that Sch-28080 at the concentration of 100 μM selectively blocked gastric H^+,K^+-ATPase and did not significantly affect other apparatuses such as Na^+,K^+-ATPase and NKCC1 (4, 5, 7, 50, 68, 85, 92), EP reduction by Sch-28080 observed in this study would be mainly attributable to suppression of the H^+,K^+-ATPase.

Putative role of gastric H^+,K^+-ATPase in cochlear stria vascularis. The cochlear stria vascularis is known playing essential roles in generation of EP (Fig. 7*A*) (83, 90). Salt et al. (65) found a unique space sandwiched between basolateral membrane of marginal cells and apical membrane of intermediate or basal cells in stria vascularis. This so-called intrastrial space (IS) is filled with an unusual extracellular fluid that contains low $[K^+]$ ($[K^+]_{IS}$) of ~1–2 mM and exhibits a highly positive potential of approximately +100 mV with reference to the body fluid (Fig. 7*B*) (31, 65). IS is electrically isolated with two tight-junction shields: the marginal cell layer and the basal cell layer (19, 33, 39, 40, 78). Intermediate and basal cells are connected through gap junctions not only to each other but also to fibrocytes, endothelial cells, and pericytes (38, 80). Thus all of these cells form an electrical syncytium, which is called the connective tissue gap-junction network (Fig. 7*B*) (38, 80). The membrane potential (E_m) of the syncytium relative to the perilymph is −5–0 mV (31, 55, 65). The apical membrane of intermediate cells is highly K^+ permeable because of abundant expression of Kir4.1 (1, 23). Takeuchi et al. (81) found that the resting membrane potential of isolated intermediate cells was almost identical to the equilibrium potential for K^+. They also examined the effects of Ba^{2+} ($[Ba^{2+}]$) in bath solution containing low $[K^+]$, similar to $[K^+]_{IS}$, on the E_m of the intermediate cells. The dependence of membrane potential changes on $[Ba^{2+}]$ was quite similar to the dependence of EP decline on $[Ba^{2+}]$ that was perfused into the artery (81). The E_m of intermediate cells may therefore directly reflect the high potential of IS and this potential as a source of EP. It is also strongly suggested that Kir4.1 is responsible for formation of the potential difference across the apical membrane of intermediate cell. This idea is also supported by the observation that Kir4.1-null mice completely lost EP (54). If Kir4.1 is the key player for establishment of the high potential of IS, the low $[K^+]_{IS}$ (1–2 mM) must be constantly maintained to form the potential difference (65, 81, 91). The NKCC1 and Na^+,K^+-ATPase that are expressed at the basolateral membrane of marginal cells are responsible for maintaining low $[K^+]_{IS}$ (Fig. 7*B*), and vascular perfusion of respective inhibitor largely reduces EP (46, 48). It is therefore possible that the H^+,K^+-ATPase localizing at the basolateral membrane of marginal cells also participates in maintenance of low $[K^+]_{IS}$ alongside NKCC1 and Na^+,K^+-ATPase.

It is rather surprising that inhibition of any one of the three K^+ transport apparatuses, Na^+,K^+-ATPase, NKCC1, and H^+,K^+-ATPase, results in reduction of EP. This very sensitive alteration in EP may be related to the features in the control of $[K^+]_{IS}$. One possibility might be associated with the morphological feature of IS. The IS between basolateral membrane of

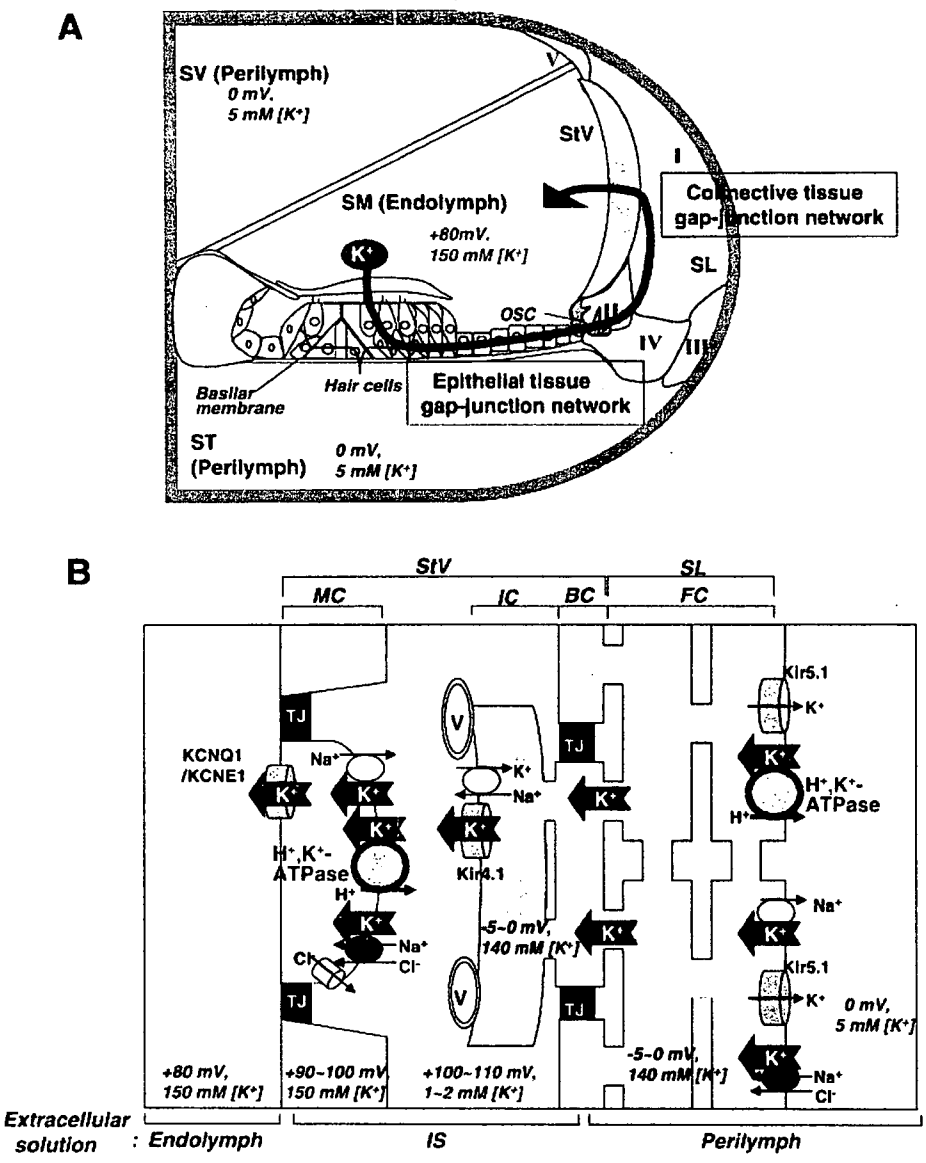

Fig. 7. Schematic model of cochlear K^+ circulation and formation of EP in the lateral wall. *A*: K^+ exiting from the hair cells is circulated to the type II and IV fibrocytes in the spiral ligament (SL) through the epithelial tissue gap-junction network, which is composed of ECs on the basilar membrane and OSC in the ligament. K^+ is taken up by types II and IV fibrocytes in the SL and then transported to the StV via the connective tissue gap-junction network, comprising the fibrocytes, basal cells, and ICs (see detail in *B*). MCs secrete K^+ across their apical membrane to maintain the endolymph. The concentration of K^+ ($[K^+]$) and the potential of each cochlear fluid are indicated. *B*: ion transport molecules expressed in the StV and the SL that participate in cochlear K^+ circulation. The potential and $[K^+]$ in each compartment are indicated. The involvement of H^+,K^+-ATPase in formation of EP and cochlear K^+ circulation is described in text. FC, fibrocytes; BC, basal cells; IS, intrastrial space; TJ, tight junction. Pink circles, Na^+,K^+-ATPase; blue circles, $Na^+,K^+,2Cl^-$ cotransporter (NKCC1); yellow cylinders, Cl^- channel.

marginal cells and apical membrane of intermediate cells is very narrow, of ~150–200Å in width (28, 72). Because of this feature, the amount of fluid in the IS should be very small, and thus $[K^+]_{IS}$ can be very easily affected by a very small alteration in K^+ inflow to IS or K^+ outflow from IS. Inhibition of any one of the K^+ transport apparatuses may thus cause significant increase in $[K^+]_{IS}$ even though accumulation of K^+ in IS is very small. Alteration in $[K^+]_{IS}$ should be directly reflected to EP, because the potential difference across the apical membrane of intermediate cells is determined by Kir4.1.

However, this may not be enough to explain why strong inhibition of any one of the H^+,K^+-ATPase, the NKCC1, and the Na^+,K^+-ATPase expressed in stria vascularis caused complete suppression of EP (Fig. 6) (46, 47). One possibility might be that, at the basolateral site of marginal cells, the three apparatuses are functionally coupled to form a complex of machinery for effective K^+ transport, and that disruption of any one of them would significantly impair K^+ transport function of the complex. Further studies are needed to clarify this possibility.

Putative role of gastric H^+,K^+-ATPase in cochlear spiral ligament. It is assumed that K^+ circulation from perilymph to endolymph through cochlear lateral wall is essential for maintaining primarily endolymphatic high $[K^+]$ and thus EP. Two functional components are considered to be critically involved in the K^+ circulation. They are the epithelial tissue and connective tissue gap junction networks (Fig. 7*A*). The former is composed of the supporting cells beneath the hair cells, the epithelial cells on basilar membrane, and the outer sulcus cells, whereas the latter comprises the fibrocytes in spiral ligament and some cells in stria vascularis, as stated above. K^+ released from the hair cells seems to be absorbed by the supporting cells and then transported to the stria vascularis via the two gap junction networks. There is no gap-junctional connection between the two networks. The type II and V fibrocytes contacting with the outer sulcus cells should therefore take up K^+ by

an active process for the K^+ circulation. The NKCC1 and the Na^+,K^+-ATPase in the fibrocytes may contribute to this process (37). Perilymphatic perfusion of K^+-free solution, which may remove the extracellular K^+ around the NKCC1 and the Na^+,K^+-ATPase and thus cause them to dysfunction, and that of the inhibitors for these K^+ uptake apparatuses dramatically reduce EP (52). This highlights a possible involvement of polarized K^+ transport via the fibrocytes in EP formation. In the present study we have shown that these particular fibrocytes also express the gastric type of the H^+,K^+-ATPase (Fig. 2, *A* and *B*) and that a specific blocker for this pump, Sch-28080, applied to perilymph, caused suppression of EP (Fig. 5, *A* and *B*). Therefore, it may be reasonable to suggest that the H^+,K^+-ATPase in the fibrocytes is also involved in K^+ transport in the ligament and thus generation of EP. The H^+,K^+-ATPase would accelerate cochlear K^+ circulation by taking up K^+ in exchange to H^+ from perilymph alongside of the NKCC1 and the Na^+,K^+-ATPase (Fig. 7*B*). This also may occur in fibrocytes in the suprastrial zone of the spiral ligament and in those of the spiral limbus, which are thought to be another pathway of K^+ transport from endolymph to perilymph (90).

Future questions and direction. In summary, we have shown that the gastric type of H^+,K^+-ATPase is abundantly expressed in cochlear stria vascularis and spiral ligament and may be critically involved in EP formation, probably through control of the K^+ circulation in the lateral wall. Several issues, however, remain to be addressed for comprehensive understanding of the roles of the H^+,K^+-ATPase in auditory function.

The H^+,K^+-ATPase extrudes H^+ in exchange to K^+ from intracellular milieu to extracellular fluid. Thus this pump also may be involved in the pH control of cochlear fluids. Whereas Sch-28080 perfused to the lateral wall largely suppressed EP, vascular or perilymphatic perfusion of omeprazole, another specific inhibitor of gastric type H^+,K^+-ATPase, did not significantly affect EP (Figs. 5 and 6). This observation may suggest that the extracellular solution in IS or in the ligament may not be acidic enough, because omeprazole is activated only in a strong acidic environment of pH <5 (51, 89). Actually, it has been reported that pH of perilymph is 7.8–8.0 (56). This may be due to the effective neutralization of the protons by HCO_3^- secreted via Cl^-/HCO_3^- exchangers expressed in the outer sulcus cells neighboring the fibrocytes (75). Although the pH value of IS solution has not yet been measured, the following observations in other tissues may support the idea that the solution would not be strongly acidic. For example, in the prostate of mice, the secretions are mildly acidic with a pH value of ~6.4. The slight acidification is, however, caused by the colonic H^+,K^+-ATPase expressed in the prostate epithelia, because the secretions are alkalinized to pH ~7 when the α_2-subunit-gene is ablated (60). In kidney, although gastric type H^+,K^+-ATPase is shown expressed in its epithelia and involved in the control of proton transport in vitro with omeprazole (17, 41), in vivo application of the inhibitor to healthy human subjects did not affect their urinary pH (29, 58). Accordingly, differently from the gastric mucosa, the primary role of H^+,K^+-ATPase in these organs, and probably also in cochlea, would be the absorption of K^+ from the extracellular fluid and the pH control of intracellular milieu rather than extracellular fluid.

However, there remains a possibility that abnormality in the proton production by the H^+,K^+-ATPase could be linked with some pathological conditions of inner ear. Indeed, venous injection of sodium bicarbonate solution is an effective therapy for vertigo and dizziness induced by different defects in the inner ear, including Méniere's disease (21). Thus the relevance of gastric type H^+,K^+-ATPase in various auditory diseases should be examined. It may therefore be of interest to examine whether the H^+,K^+-ATPase-null mice (61, 62, 74) exhibit hearing disorder or whether there are hereditary or sporadic mutations of the gene encoding the ATPase in deaf patients. Further studies on the subjects described above are needed to clarify the physiological and pathological roles of the H^+,K^+-ATPase in cochlea.

ACKNOWLEDGMENTS

We thank Dr. Ian Findlay (Université de Tours, Tours, France) for critically reading this manuscript.

GRANTS

This work was supported by the following research grants and funding: Grant-in-Aid for Scientific Research on Priority Areas (2) 12144207 (to Y. Kurachi), Grant-in-Aid for Scientific Research on Priority Areas 17081012 (to H. Hibino), Grant-in-Aid for Young Scientists (A) 17689012 (to H. Hibino), and Japan-France Integrated Action Program (SAKURA) (to Y. Kurachi) from the Ministry of Education, Science, Sports and Culture of Japan, and the Uehara Memorial Foundation (to Y. Kurachi), Kanae Foundation for Life & Socio-Medical Science (to H. Hibino), Inamori Foundation (to H. Hibino), and Yamanouchi Foundation for Research on Metabolic Disorders (to H. Hibino).

REFERENCES

1. **Ando M and Takeuchi S.** Immunological identification of an inward rectifier K^+ channel (Kir4.1) in the intermediate cell (melanocyte) of the cochlear stria vascularis of gerbils and rats. *Cell Tissue Res* 298: 179–183, 1999.
2. **Asano S, Arakawa S, Hirasawa M, Sakai H, Ohta M, Ohta K, and Takeguchi N.** C-terminal topology of gastric H^+,K^+-ATPase. *Biochem J* 299: 59–64, 1994.
3. **Asano S, Morii M, and Takeguchi N.** Molecular and cellular regulation of the gastric proton pump. *Biol Pharm Bull* 27: 1–12, 2004.
4. **Beil W, Hackbarth I, and Sewing KF.** Mechanism of gastric antisecretory effect of SCH 28080. *Br J Pharmacol* 88: 19–23, 1986.
5. **Beisvag V, Falck G, Loennechen JP, Qvigstad G, Jynge P, Skomedal T, Osnes JB, Sandvik AK, and Ellingsen O.** Identification and regulation of the gastric H^+/K^+-ATPase in the rat heart. *Acta Physiol Scand* 179: 251–262, 2003.
6. **Cable J, Barkway C, and Steel KP.** Characteristics of stria vascularis melanocytes of viable dominant spotting (W^v/W^v) mouse mutants. *Hear Res* 64: 6–20, 1992.
7. **Cheval L, Barlet-Bas C, Khadouri C, Feraille E, Marsy S, and Doucet A.** K^+-ATPase-mediated Rb^+ transport in rat collecting tubule: modulation during K^+ deprivation. *Am J Physiol Renal Fluid Electrolyte Physiol* 260: F800–F805, 1991.
8. **Codina J, Delmas-Mata JT, and DuBose TD Jr.** The α-subunit of the colonic H^+,K^+-ATPase assembles with β_1-Na^+,K^+-ATPase in kidney and distal colon. *J Biol Chem* 273: 7894–7899, 1998.
9. **Codina J, Kone BC, Delmas-Mata JT, and DuBose TD Jr.** Functional expression of the colonic H^+,K^+-ATPase α-subunit. Pharmacologic properties and assembly with X^+,K^+-ATPase β-subunits. *J Biol Chem* 271: 29759–29763, 1996.
10. **Cohen-Salmon M, Ott T, Michel V, Hardelin JP, Perfettini I, Eybalin M, Wu T, Marcus DC, Wangemann P, Willecke K, and Petit C.** Targeted ablation of connexin26 in the inner ear epithelial gap junction network causes hearing impairment and cell death. *Curr Biol* 12: 1106–1111, 2002.
11. **Crouch JJ, Sakaguchi N, Lytle C, and Schulte BA.** Immunohistochemical localization of the Na-K-Cl co-transporter (NKCC1) in the gerbil inner ear. *J Histochem Cytochem* 45: 773–778, 1997.
12. **Dechesne CJ, Kim HN, Nowak TS Jr, and Wenthold RJ.** Expression of heat shock protein, HSP72, in the guinea pig and rat cochlea after hyperthermia: immunochemical and in situ hybridization analysis. *Hear Res* 59: 195–204, 1992.
13. **Denoyelle F, Marlin S, Weil D, Moatti L, Chauvin P, Garabedian EN, and Petit C.** Clinical features of the prevalent form of childhood deafness,

DFNB1, due to a connexin-26 gene defect: implications for genetic counseling. *Lancet* 353: 1298–1303, 1999.
14. **DuBose TD Jr, Gitomer J, and Codina J.** H^+,K^+-ATPase. *Curr Opin Nephrol Hypertens* 8: 597–602, 1999.
15. **Estevez R, Boettger T, Stein V, Birkenhager R, Otto E, Hildebrandt F, and Jentsch TJ.** Barttin is a Cl^- channel β-subunit crucial for renal Cl^- reabsorption and inner ear K^+ secretion. *Nature* 414: 558–561, 2001.
16. **Fujita A, Horio Y, Higashi K, Mouri T, Hata F, Takeguchi N, and Kurachi Y.** Specific localization of an inwardly rectifying K^+ channel, Kir4.1, at the apical membrane of rat gastric parietal cells; its possible involvement in K^+ recycling for the H^+-K^+-pump. *J Physiol* 540: 85–92, 2002.
17. **Garg LC and Narang N.** Ouabain-insensitive K-adenosine triphosphatase in distal nephron segments of the rabbit. *J Clin Invest* 81: 1204–1208, 1988.
18. **Goto S, Oshima T, Ikeda K, Ueda N, and Takasaka T.** Expression and localization of the Na-K-2Cl cotransporter in the rat cochlea. *Brain Res* 765: 324–326, 1997.
19. **Gow A, Davies C, Southwood CM, Frolenkov G, Chrustowski M, Ng L, Yamauchi D, Marcus DC, and Kachar B.** Deafness in Claudin 11-null mice reveals the critical contribution of basal cell tight junctions to stria vascularis function. *J Neurosci* 24: 7051–7062, 2004.
20. **Hall K, Perez G, Anderson D, Gutierrez C, Munson K, Hersey SJ, Kaplan JH, and Sachs G.** Location of the carbohydrates present in the HK-ATPase vesicles isolated from hog gastric mucosa. *Biochemistry* 29: 701–706, 1990.
21. **Hasegawa T.** Intravenous injection Of 7 percent solution of sodium-bicarbonate for the treatment of Méniere's disease. *Acta Otolaryngol Suppl* 192: 113+, 1963.
22. **Hibino H, Fujita A, Iwai K, Yamada M, and Kurachi Y.** Differential assembly of inwardly rectifying K^+ channel subunits, Kir4.1 and Kir5.1, in brain astrocytes. *J Biol Chem* 279: 44065–44073, 2004.
23. **Hibino H, Higashi-Shingai K, Fujita A, Iwai K, Ishii M, and Kurachi Y.** Expression of an inwardly rectifying K^+ channel, Kir5.1, in specific types of fibrocytes in the cochlear lateral wall suggests its functional importance in the establishment of endocochlear potential. *Eur J Neurosci* 19: 76–84, 2004.
24. **Hibino H, Horio Y, Inanobe A, Doi K, Ito M, Yamada M, Gotow T, Uchiyama Y, Kawamura M, Kubo T, and Kurachi Y.** An ATP-dependent inwardly rectifying potassium channel, K_{AB}-2 (Kir4.1), in cochlear stria vascularis of inner ear: its specific subcellular localization and correlation with the formation of endocochlear potential. *J Neurosci* 17: 4711–4721, 1997.
25. **Hibino H, Pironkova R, Onwumere O, Rousset M, Charnet P, Hudspeth AJ, and Lesage F.** Direct interaction with a nuclear protein and regulation of gene silencing by a variant of the Ca^{2+}-channel β_4 subunit. *Proc Natl Acad Sci USA* 100: 307–312, 2003.
26. **Higashi K, Fujita A, Inanobe A, Tanemoto M, Doi K, Kubo T, and Kurachi Y.** An inwardly rectifying K^+ channel, Kir4.1, expressed in astrocytes surrounds synapses and blood vessels in brain. *Am J Physiol Cell Physiol* 281: C922–C931, 2001.
27. **Hilding DA and Ginzberg RD.** Pigmentation of the stria vascularis. The contribution of neural crest melanocytes. *Acta Otolaryngol* 84: 24–37, 1977.
28. **Hinojosa R and Rodriguez-Echandia EL.** The fine structure of the stria vascularis of the cat inner ear. *Am J Anat* 118: 631–663, 1966.
29. **Howden CW and Reid JL.** Omeprazole, a gastric "proton pump inhibitor": lack of effect on renal handling of electrolytes and urinary acidification. *Eur J Clin Pharmacol* 26: 639–640, 1984.
30. **Hudspeth AJ.** How hearing happens. *Neuron* 19: 947–950, 1997.
31. **Ikeda K and Morizono T.** Electrochemical profiles for monovalent ions in the stria vascularis: cellular model of ion transport mechanisms. *Hear Res* 39: 279–286, 1989.
32. **Ishii M, Fujita A, Iwai K, Kusaka S, Higashi K, Inanobe A, Hibino H, and Kurachi Y.** Differential expression and distribution of Kir5.1 and Kir4.1 inwardly rectifying K^+ channels in retina. *Am J Physiol Cell Physiol* 285: C260–C267, 2003.
33. **Jahnke K.** The fine structure of freeze-fractured intercellular junctions in the guinea pig inner ear. *Acta Otolaryngol Suppl* 336: 1–40, 1975.
34. **Kakigi A, Takeuchi S, Ando M, Higashiyama K, Azuma H, Sato T, and Takeda T.** Reduction in the endocochlear potential caused by Cs^+ in the perilymph can be explained by the five-compartment model of the stria vascularis. *Hear Res* 166: 54–61, 2002.
35. **Kelsell DP, Dunlop J, Stevens HP, Lench NJ, Liang JN, Parry G, Mueller RF, and Leigh IM.** Connexin 26 mutations in hereditary non-syndromic sensorineural deafness. *Nature* 387: 80–83, 1997.
36. **Kerr TP, Ross MD, and Ernst SA.** Cellular localization of Na^+,K^+-ATPase in the mammalian cochlear duct: significance for cochlear fluid balance. *Am J Otolaryngol* 3: 332–338, 1982.
37. **Kikuchi T, Adams JC, Miyabe Y, So E, and Kobayashi T.** Potassium ion recycling pathway via gap junction systems in the mammalian cochlea and its interruption in hereditary nonsyndromic deafness. *Med Electron Microsc* 33: 51–56, 2000.
38. **Kikuchi T, Kimura RS, Paul DL, and Adams JC.** Gap junctions in the rat cochlea: immunohistochemical and ultrastructural analysis. *Anat Embryol (Berl)* 191: 101–118, 1995.
39. **Kitajiri S, Miyamoto T, Mineharu A, Sonoda N, Furuse K, Hata M, Sasaki H, Mori Y, Kubota T, Ito J, Furuse M, and Tsukita S.** Compartmentalization established by claudin-11-based tight junctions in stria vascularis is required for hearing through generation of endocochlear potential. *J Cell Sci* 117: 5087–5096, 2004.
40. **Kitajiri SI, Furuse M, Morita K, Saishin-Kiuchi Y, Kido H, Ito J, and Tsukita S.** Expression patterns of claudins, tight junction adhesion molecules, in the inner ear. *Hear Res* 187: 25–34, 2004.
41. **Kleinman JG.** Proton ATPases and urinary acidification. *J Am Soc Nephrol* 5: S6–11, 1994.
42. **Kobayashi T, Rokugo M, Marcus DC, Comegys TH, and Thalmann R.** Prolonged maintenance of endocochlear potential by vascular perfusion with media devoid of oxygen carriers. *Arch Otorhinolaryngol* 239: 243–247, 1984.
43. **Konishi T and Mendelsohn M.** Effect of ouabain on cochlear potentials and endolymph composition in guinea pigs. *Acta Otolaryngol* 69: 192–199, 1970.
44. **Konno T, Watanabe J, and Ishihara K.** Enhanced solubility of paclitaxel using water-soluble and biocompatible 2-methacryloyloxyethyl phosphorylcholine polymers. *J Biomed Mater Res A* 65: 209–214, 2003.
45. **Kraut JA, Hiura J, Shin JM, Smolka A, Sachs G, and Scott D.** The Na^+-K^+-ATPase β_1 subunit is associated with the $HK\alpha_2$ protein in the rat kidney. *Kidney Int* 53: 958–962, 1998.
46. **Kuijpers W.** Cation transport and cochlear function. *Acta Otolaryngol* 67: 200–205, 1969.
47. **Kusakari J, Ise I, Comegys TH, Thalmann I, and Thalmann R.** Effect of ethacrynic acid, furosemide, and ouabain upon the endolymphatic potential and upon high energy phosphates of the stria vascularis. *Laryngoscope* 88: 12–37, 1978.
48. **Kusakari J, Kambayashi J, Ise I, and Kawamoto K.** Reduction of the endocochlear potential by the new "loop" diuretic, bumetanide. *Acta Otolaryngol* 86: 336–341, 1978.
49. **Lecain E, Robert JC, Thomas A, and Tran Ba Huy P.** Gastric proton pump is expressed in the inner ear and choroid plexus of the rat. *Hear Res* 149: 147–154, 2000.
50. **Leyssens A, Dijkstra S, Van Kerkhove E, and Steels P.** Mechanisms of K^+ uptake across the basal membrane of malpighian tubules of *Formica polyctena*: the effect of ions and inhibitors. *J Exp Biol* 195: 123–145, 1994.
51. **Lorentzon P, Eklundh B, Brandstrom A, and Wallmark B.** The mechanism for inhibition of gastric (H^+ + K^+)-ATPase by omeprazole. *Biochim Biophys Acta* 817: 25–32, 1985.
52. **Marcus DC, Marcus NY, and Thalmann R.** Changes in cation contents of stria vascularis with ouabain and potassium-free perfusion. *Hear Res* 4: 149–160, 1981.
53. **Marcus DC, Rokugo M, and Thalmann R.** Effects of barium and ion substitutions in artificial blood on endocochlear potential. *Hear Res* 17: 79–86, 1985.
54. **Marcus DC, Wu T, Wangemann P, and Kofuji P.** KCNJ10 (Kir4.1) potassium channel knockout abolishes endocochlear potential. *Am J Physiol Cell Physiol* 282: C403–C407, 2002.
55. **Melichar I and Syka J.** Electrophysiological measurements of the stria vascularis potentials in vivo. *Hear Res* 25: 35–43, 1987.
56. **Misrahy GA, Hildreth KM, Clark LC, and Shinabarger EW.** Measurement of the pH of the endolymph in the cochlea of guinea pigs. *Am J Physiol* 194: 393–395, 1958.
57. **Mizuta K, Adachi M, and Iwasa KH.** Ultrastructural localization of the Na-K-Cl cotransporter in the lateral wall of the rabbit cochlear duct. *Hear Res* 106: 154–162, 1997.
58. **Osther PJ, Rasmussen L, and Pedersen SA.** A double-blind placebo-controlled trial of omeprazole on urinary pH in healthy subjects. *Int Urol Nephrol* 24: 229–231, 1992.

59. **Pestov NB, Korneenko TV, Radkov R, Zhao H, Shakhparonov MI, and Modyanov NN.** Identification of the β-subunit for nongastric H-K-ATPase in rat anterior prostate. *Am J Physiol Cell Physiol* 286: C1229–C1237, 2004.
60. **Pestov NB, Korneenko TV, Shakhparonov MI, Shull GE, and Modyanov NN.** Loss of acidification of anterior prostate fluids in *Atp12A* null mutant mice indicates that the nongastric H,K-ATPase functions as a proton pump in vivo. *Am J Physiol Cell Physiol* 291: C366–C374, 2006.
61. **Petrovic S, Spicer Z, Greeley T, Shull G.E, and Soleimani M.** Novel Schering and ouabain-insensitive potassium-dependent proton secretion in the mouse cortical collecting duct. *Am J Physiol Renal Physiol* 282: F133–F143, 2002.
62. **Petrovic S, Wang Z, Ma L, Seidler U, Forte JG, Shull GE, and Soleimani M.** Colocalization of the apical Cl^-/HCO_3^- exchanger PAT1 and gastric H-K-ATPase in stomach parietal cells. *Am J Physiol Gastrointest Liver Physiol* 283: G1207–G1216, 2002.
63. **Sachs G, Shin JM, Briving C, Wallmark B, and Hersey S.** The pharmacology of the gastric acid pump: the H^+,K^+ ATPase. *Annu Rev Pharmacol Toxicol* 35: 277–305, 1995.
64. **Sakagami M, Fukazawa K, Matsunaga T, Fujita H, Mori N, Takumi T, Ohkubo H, and Nakanishi S.** Cellular localization of rat Isk protein in the stria vascularis by immunohistochemical observation. *Hear Res* 56: 168–172, 1991.
65. **Salt AN, Melichar I, and Thalmann R.** Mechanisms of endocochlear potential generation by stria vascularis. *Laryngoscope* 97: 984–991, 1987.
66. **Schlatter E, Greger R, and Weidtke C.** Effect of "high ceiling" diuretics on active salt transport in the cortical thick ascending limb of Henle's loop of rabbit kidney. Correlation of chemical structure and inhibitory potency. *Pflügers Arch* 396: 210–217, 1983.
67. **Schulte BA and Adams JC.** Distribution of immunoreactive Na^+,K^+-ATPase in gerbil cochlea. *J Histochem Cytochem* 37: 127–134, 1989.
68. **Scott CK, Sundell E, and Castrovilly L.** Studies on the mechanism of action of the gastric microsomal (H^+ + K^+)-ATPase inhibitors SCH 32651 and SCH 28080. *Biochem Pharmacol* 36: 97–104, 1987.
69. **Shindo M, Miyamoto M, Abe N, Shida S, Murakami Y, and Imai Y.** Dependence of endocochlear potential on basolateral Na^+ and Cl^- concentration: a study using vascular and perilymph perfusion. *Jpn J Physiol* 42: 617–630, 1992.
70. **Silver RB and Soleimani M.** H^+-K^+-ATPases: regulation and role in pathophysiological states. *Am J Physiol Renal Physiol* 276: F799–F811, 1999.
71. **Spicer SS and Schulte BA.** The fine structure of spiral ligament cells relates to ion return to the stria and varies with place-frequency. *Hear Res* 100: 80–100, 1996.
72. **Spicer SS and Schulte BA.** Novel structures in marginal and intermediate cells presumably relate to functions of apical versus basal strial strata. *Hear Res* 200: 87–101, 2005.
73. **Spicer SS and Schulte BA.** Spiral ligament pathology in quiet-aged gerbils. *Hear Res* 172: 172–185, 2002.
74. **Spicer Z, Miller ML, Andringa A, Riddle TM, Duffy JJ, Doetschman T, and Shull GE.** Stomachs of mice lacking the gastric H,K-ATPase α-subunit have achlorhydria, abnormal parietal cells, and ciliated metaplasia. *J Biol Chem* 275: 21555–21565, 2000.
75. **Stankovic KM, Brown D, Alper SL, and Adams JC.** Localization of pH regulating proteins H^+ATPase and Cl^-/HCO_3^- exchanger in the guinea pig inner ear. *Hear Res* 114: 21–34, 1997.
76. **Steel KP, Barkway C, and Bock GR.** Strial dysfunction in mice with cochleo-saccular abnormalities. *Hear Res* 27: 11–26, 1987.
77. **Suvitayavat W, Palfrey HC, Haas M, Dunham PB, Kalmar F, and Rao MC.** Characterization of the endogenous Na^+-K^+-$2Cl^-$ cotransporter in *Xenopus* oocytes. *Am J Physiol Cell Physiol* 266: C284–C292, 1994.
78. **Suzuki T, Oyamada M, and Takamatsu T.** Different regulation of connexin26 and ZO-1 in cochleas of developing rats and of guinea pigs with endolymphatic hydrops. *J Histochem Cytochem* 49: 573–586, 2001.
79. **Suzuki T, Takamatsu T, and Oyamada M.** Expression of gap junction protein connexin43 in the adult rat cochlea: comparison with connexin26. *J Histochem Cytochem* 51: 903–912, 2003.
80. **Takeuchi S and Ando M.** Dye-coupling of melanocytes with endothelial cells and pericytes in the cochlea of gerbils. *Cell Tissue Res* 293: 271–275, 1998.
81. **Takeuchi S, Ando M, and Kakigi A.** Mechanism generating endocochlear potential: role played by intermediate cells in stria vascularis. *Biophys J* 79: 2572–2582, 2000.
82. **Takeuchi S, Ando M, Kozakura K, Saito H, and Irimajiri A.** Ion channels in basolateral membrane of marginal cells dissociated from gerbil stria vascularis. *Hear Res* 83: 89–100, 1995.
83. **Tasaki I and Spyropoulos CS.** Stria vascularis as source of endocochlear potential. *J Neurophysiol* 22: 149–155, 1959.
84. **Tranebjaerg L, Bathen J, Tyson J, and Bitner-Glindzicz M.** Jervell and Lange-Nielsen syndrome: a Norwegian perspective. *Am J Med Genet* 89: 137–146, 1999.
85. **Tsukimi Y, Ushiro T, Yamazaki T, Ishikawa H, Hirase J, Narita M, Nishigaito T, Banno K, Ichihara T, and Tanaka H.** Studies on the mechanism of action of the gastric H^+,K^+-ATPase inhibitor SPI-447. *Jpn J Pharmacol* 82: 21–28, 2000.
86. **Von Bekesy G.** DC resting potentials inside the cochlear partition. *J Acoust Soc Am* 24: 72–76, 1952.
87. **Von Bekesy G.** Resting potentials inside the cochlear partition of the guinea pig. *Nature* 169: 241–242, 1952.
88. **Wallmark B, Briving C, Fryklund J, Munson K, Jackson R, Mendlein J, Rabon E, and Sachs G.** Inhibition of gastric H^+,K^+-ATPase and acid secretion by SCH 28080, a substituted pyridyl(1,2*a*)imidazole. *J Biol Chem* 262: 2077–2084, 1987.
89. **Wallmark B, Jaresten BM, Larsson H, Ryberg B, Brandstrom A, and Fellenius E.** Differentiation among inhibitory actions of omeprazole, cimetidine, and SCN- on gastric acid secretion. *Am J Physiol Gastrointest Liver Physiol* 245: G64–G71, 1983.
90. **Wangemann P.** K^+ cycling and the endocochlear potential. *Hear Res* 165: 1–9, 2002.
91. **Wangemann P, Liu J, and Marcus DC.** Ion transport mechanisms responsible for K^+ secretion and the transepithelial voltage across marginal cells of stria vascularis in vitro. *Hear Res* 84: 19–29, 1995.
92. **Younes-Ibrahim M, Barlet-Bas C, Buffin-Meyer B, Cheval L, Rajerison R, and Doucet A.** Ouabain-sensitive and -insensitive K-ATPases in rat nephron: effect of K depletion. *Am J Physiol Renal Fluid Electrolyte Physiol* 268: F1141–F1147, 1995.

Journal of Neuroscience Research 83:1573–1583 (2006)

Fos-Enkephalin Signaling in the Rat Medial Vestibular Nucleus Facilitates Vestibular Compensation

Tadashi Kitahara,[1]* Takeshi Kaneko,[2] Arata Horii,[1] Munehisa Fukushima,[1] Kaoru Kizawa-Okumura,[1] Noriaki Takeda,[3] and Takeshi Kubo[1]

[1]Department of Otolaryngology, Osaka University, School of Medicine, Osaka, Japan
[2]Department of Morphological Brain Science, Kyoto University, School of Medicine, Kyoto, Japan
[3]Department of Otolaryngology, Tokushima University, School of Medicine, Tokushima, Japan

In the present study, we first observed up-regulation in preproenkephalin (PPE)-like immunoreactivity (-LIR), a precursor of Met- and Leu-enkephalin, in the rat ipsilateral medial vestibular nucleus (ipsi-MVN) after unilateral labyrinthectomy (UL). By means of double-staining immunohistochemistry with PPE and Fos, a putative regulator of PPE gene expression, we revealed that some of these PPE-LIR neurons were also Fos immunopositive. The time course of decay of these double-stained neurons was quite parallel to that of UL-induced behavioral deficits. This suggests that these double-labeled neurons could have something to do with development of vestibular compensation. We next examined correlation between Fos and PPE expression in the ipsi-MVN by means of a 15-min pre-UL application of antisense oligonucleotide probes against c-fos mRNA into the ipsi-MVN. Gel shift assay and Western blotting revealed that elimination of Fos expression significantly reduced both AP-1 DNA binding activity and PPE expression in the ipsi-MVN after UL. C-fos antisense study also revealed that depression of Fos-PPE signaling in the ipsi-MVN caused significantly more severe behavioral deficits during vestibular compensation. Furthermore, studies with PPE antisense and naloxone, an opioid receptor antagonist, demonstrated that specific depression of enkephalinergic effects in the ipsi-MVN significantly delayed vestibular compensation. All these findings suggest that, immediately after UL, Fos induced in some of the ipsi-MVN neurons could regulate consequent PPE expression via the AP-1 activation and facilitate the restoration of balance between bilateral MVN activities via the opioid receptor activation, resulting in progress of vestibular compensation. © 2006 Wiley-Liss, Inc.

Key words: labyrinthectomy; Bechterew's phenomenon; Fos; preproenkephalin; medial vestibular nucleus; antisense oligonucleotides; gel shift assay

Unilateral labyrinthectomy (UL) induces severe postural and oculomotor asymmetry, such as barrel rotation, head tilt, and spontaneous nystagmus. However, these functional deficits recover gradually after the lesion without any vestibular peripheral regeneration. This phenomenon is referred to as *vestibular compensation* (Llinas and Walton, 1979; Precht and Dieringer, 1985; Aldrich and Peusner, 2002) and has been used as a model of lesion-induced neuronal plasticity in the central nervous system.

Several lines of evidence have suggested that enkephalin, one of the major opiates in the central nervous system, is a possible neurotransmitter/neuromodulator involved in the central vestibular system. It was reported that UL induced up-regulation of preproenkephalin (PPE) mRNA, a precursor of Met- and Leu-enkephalin, in the ipsilateral medial vestibular nucleus (ipsi-MVN) neurons, and the decay profile of PPE mRNA expression was quite related to that of vestibular deficits after UL (Saika et al., 1993). However, the systemic administration of naloxone, an opioid receptor antagonist, enhanced vestibuloocular compensation (Dutia et al., 1996). Furthermore, whereas opiates directly activate the MVN neurons (Lin and Carpenter, 1994), δ-opioid receptors demonstrate inhibitory effects on the MVN neurons (Sulaiman and Dutia, 1998). So far, the parts of the central nervous system in which enkephalinergic neurons have effects on (or how these effects act on) central vestibular neuronal plasticity have not been determined.

The aim in the present study is to elucidate the role of preproenkephalinergic neurons in the central vestibular system during vestibular compensation. We first examined changes in PPE-like immunoreactivity (-LIR) in the rat brainstem after UL and after two-staged bilateral labyrinthectomy (BL) compared with those in lesion-induced behavioral deficits. So far, we have focused on UL-induced Fos expression in the ipsi-MVN in the hope of understanding neuronal circuits associated with vestib-

*Correspondence to: Tadashi Kitahara, MD, PhD, Department of Otolaryngology, Osaka University School of Medicine, 2-2 Yamadaoka, Suita, Osaka 565-0871, Japan. E-mail: tkitahara@ent.med.osaka-u.ac.jp

Received 4 January 2006; Revised 26 January 2006; Accepted 27 January 2006

Published online 17 March 2006 in Wiley InterScience (www.interscience.wiley.com). DOI: 10.1002/jnr.20830

ular compensation (Kitahara et al., 1995, 1997, 2002; Fukushima et al., 2001). Nuclear Fos protein is one of the immediately early genes and also well known to bind and activate a DNA binding site called AP-1, which is located in the PPE promoter region (Sonnenberg et al., 1989). Therefore, we next examined effects of Fos-PPE signaling in the ipsi-MVN after UL on vestibular compensation by using antisense oligonucleotide probes against c-fos or PPE mRNA.

MATERIALS AND METHODS

All procedures were approved by the Animal Care and Use Committee at Osaka University Graduate School of Medicine, Japan. All efforts were made to minimize the numbers of animals used and their suffering.

UL and BL

Adult Wistar rats (Japan Clea), weighing about 150 g, were anesthetized with ether inhalation. The right bulla was exposed on one side by blunt dissection via a skin incision near the angle of the mandible, and a pediatric otic speculum was placed over the bone to maintain retraction of soft tissues. The ventral surface of the bulla was removed with a fine dental burr and microrongeurs to expose the middle ear cavity. The base of the cochlea was opened with a dental burr and small picks to expose the vestibule and the otolith organs, and the semicircular canal cristae were ablated with a curette and aspiration. This procedure ablates the neuroepithelium, without involvement of the ossicular chain, tympanic membrane, internal acoustic canal, cochlear nerve, facial nerve, or Scarpa's ganglion (Goto et al., 1997). At the end of surgery, antibiotic cream (Furacin) was topically applied to the opened labyrinth to prevent infection, and the temporal bone was sealed with dental cement. The operative wound was sutured and the animal allowed to recover in light. Histological examination after labyrinthectomy showed that the surgical destruction of the membranous labyrinth had been achieved and that no vestibular hair cells had regenerated (data not shown).

At each post-UL interval of 6 hr, 1 day, 3 days, 1 week, or 2 weeks, four animals were deeply anesthetized with sodium pentobarbital (60 mg/kg, i.p.) and transcardially perfused with 100 ml ice-cold saline, followed by 250 ml Zamboni's fixative (4% paraformaldehyde and 0.2% picric acid in 0.1 M PBS, pH 7.4; UL group). Sham-operated animals were used as controls (n = 4).

At each post-UL interval of 0 hr (simultaneous BL), 3 days, 1 week, or 2 weeks, four animals received left labyrinthectomies. One day after the second surgery, animals were deeply anesthetized with sodium pentobarbital (60 mg/kg, i.p.) and transcardially perfused with 100 ml ice-cold saline, followed by 250 ml of the fixative mentioned above (BL group).

Immunohistochemistry Via ABC Method

The avidin-biotin complex (ABC) method was used to visualize PPE and Fos protein expression after UL and BL. Briefly, sections were incubated sequentially in the following solutions at 4°C: 1% bovine serum albumin (BSA) and normal goat serum (NGS) in 0.3% Triton X-100 in PBS for 3 hr, antisera against PPE kindly gifted from Prof. Takeshi Kaneko (Department of Morphological Brain Science, Kyoto University; diluted 1:500; Lee et al., 1997) and Fos purchased from Oncogene Science (diluted 1:500; Delogni et al., 1988) in 1% BSA and NGS in 0.3% Triton X-100 in PBS for 48 hr, 0.1 M PBS for 15 min, biotinylated goat anti-rabbit IgG (diluted 1:250; Vector Labs., Inc.) in 1% BSA and NGS in 0.3% Triton X-100 in PBS for 24 hr, 0.1 M PBS for 15 min, Vectastain reagent (diluted 1:500; Vector, Burlingame, CA) for 24 hr, and diaminobenzidine tetrahydrochloride (DAB)/H_2O_2 for approximately 4 min and then were examined under a light microscope. Because the DAB reaction can vary in different animals and in different sections from the same animal, all the sections in which the DAB reactions were to be compared with one another were taken into the same process of immunohistochemistry at once.

Cell Counting

To detect PPE- and Fos-LIR cells after UL and BL, transverse 12-μm-thick brainstem sections were examined under a brightfield microscope at ×40 and ×100 magnification. The mean intensity of five different squares (0.5 × 0.5 μm^2) in the same cell was calculated by using a digital image analysis system (Universal Imaging Software, Japan) and compared with that in the tissue background. Only cells that had significant intensity, above the background, of DAB reaction product in cell somata were counted as PPE immunopositive. The DAB reaction product in cell somata in the MVN of sham-operated animals was adopted as the background for PPE-LIR. Similarly, only cells that had significant intensity of DAB reaction product in nuclei were counted as Fos immunopositive. The DAB reaction product in nuclei in the MVN of sham operated animals was adopted as the background for Fos-LIR. We counted the numbers of PPE-LIR and Fos-LIR cells in the ipsi-MVN through the rostral (bregma: −10.50 mm) and caudal (bregma: −13.00 mm) parts of the MVN according to a brain atlas (Paxinos and Watson, 1986). To prevent double counts, we adopted an edge-effects-unbiased cell counting method (Gundersen, 1978).

Antisense Oligonucleotide Experiments

Sixteen mer phosphorothioate oligodeoxynucleotides were synthesized on an Applied Biosystems 381A DNA synthesizer and purified by a Hitachi high-pressure liquid chromatography unit (Hitachi, Tokyo, Japan). The antisense probes against c-fos mRNA (residues 128–143; Genbank X06769) and PPE mRNA (residues 118–133; Genbank S49491) were designed as described by Ziolkowska et al. (1998) and Nicot et al. (1997), respectively.

For injections into the ipsi-MVN, a posterior surgical approach was adopted. After ether inhalation anesthesia, the posterior part of the bone situated under the occipital crest was removed and the dura incised. After lifting of the caudal part of cerebellum with a spatula, the IVth ventricle was exposed. A glass micropipette (length 56 mm, diameter 26 ga.) connected to a 1-μl Hamilton syringe (Sigma) was inserted to inject 0.5 μl of 50 μM of each antisense probe (diluted 1:1 by trypan blue) into the brain tissue of the ipsi-MVN adjacent to

the IVth ventricle 15 min before UL (against c-fos mRNA: n = 8; against PPE mRNA: n = 8). As controls, 0.5 μl of saline vehicle (n = 8) and random sequence 20 mer oligonucleotides (diluted 1:1 by trypan blue; n = 8) were injected into the ipsi-MVN 15 min before UL. As antagonist, 0.5 μl of 100 nM of naloxone (Sigma, St. Louis, MO; diluted 1:1 by trypan blue) was also injected into the ipsi-MVN 15 min before UL (n = 8) according to a previous report (Tokuyama et al., 2001).

To confirm these injection sites in the ipsi-MVN in each animal, we checked trypan blue on the transverse sections between the rostral (bregma: −10.50 mm) and caudal the (bregma: −13.00 mm) levels under a light microscope (Paxinos and Watson, 1986). Trypan blue (Sigma) was reported to be quite available and harmless for this kind of antisense experiment (Kaufman et al., 1999).

Western Blotting

Samples of the ipsi-MVN were obtained from antisense-treated (against c-fos mRNA: n = 8; against PPE mRNA: n = 8) and control (saline vehicle: n = 8; random oligonucleotides: n = 8) animals 6 hr after UL and stored at −70°C. These samples were cut on a cryostat at −20°C and trimmed to include only the ipsi-MVN tissues between genual (bregma: −10.50 mm) and hypoglossal (bregma: −13.00 mm) levels under a surgical microscope (Paxinos and Watson, 1986).

For each group, samples were homogenized on ice with a polytron homogenizer (PCU-11; Kinematica) in 20 mM HEPES (pH 7.2), 25 mM NaCl, 2 mM EGTA, 50 mM NaF, 1 mM Na_3VO_4, 25 mM β-glycerophosphate, 0.2 mM dithiothreitol (DTT), 1 mM phenylmethylsulfonyl fluoride (PMSF), 60 μg/ml aprotinin, 2 μg/ml leupeptin, and 0.1% Triton X-100. After incubation at 4°C for 30 min, homogenates were sonicated (Sonifier 250; Branson Ultrasonics) on ice for 1 min and centrifuged at 10,000*g* at 4°C for 30 min. The supernatant was removed (cytoplasmic fraction for PPE), and the pellet was rehomogenized in ice-cold lysis buffer containing 1% Triton X-100, left on ice for 30 min, and centrifuged, and the supernatant was collected (nuclear fraction for pCREB and Fos). Protein concentrations of these supernatants were measured with a protein assay kit (Pierce, Rockford, IL). Gel samples were prepared by adding sample buffer, containing final concentrations of 50 mM Tris (pH 6.7), 2% sodium dodecyl sulfate (SDS), and 2% mercaptoethanol. Twenty micrograms of protein extracts were boiled for 10 min, cooled to RT, and loaded on 10% SDS-polyacrylamide gels. Equal amounts of protein in each sample were further checked by immunoblotting with β-actin monoclonal antibody (Oncogene Research Products; diluted 1:500).

Proteins were transferred to Hybond-PVDF membranes (Amersham, Arlington Heights, IL) by using standard electroblotting procedures. Membranes were incubated sequentially in the following solutions at 4°C: 2% nonfat dry milk, 1% BSA and NGS in 0.3% Triton X-100 in PBS for 3 hr; antisera against pCREB (phosphorylated form of cAMP/calcium response element binding protein), a transcription factor for immediate early genes, including Fos (Kim et al., 2000), obtained from Calbiochem (La Jolla, CA; diluted 1:200) in addition to PPE (diluted 1:250) and Fos (diluted 1:200) in 1% BSA and NGS in 0.3% Triton X-100 in PBS for 24 hr; 0.1 M PBS for 30 min; horseradish peroxidase (HRP)-conjugated secondary antibody (Dako, Carpinteria, CA) in 1% BSA and NGS in 0.3% Triton X-100 in PBS for 3 hr; 0.1 M PBS for 30 min. Protein bands were visualized by using an ECL detection kit and Hyperfilm MP (Amersham) and analyzed in Scion Image software (Scion Corp. Frederick, MD).

Gel Shift Assay

For gel shift assay, portions of the previous samples used for Western blotting were used. Samples were homogenized in 20 mM HEPES (pH 7.9) containing 0.4 M NaCl, 1 mM EDTA, 1 mM EGTA, 1.5 mM $MgCl_2$, 20% glycerol, 10 mM NaF, 1 mM Na_3VO_4, 0.2 mM DTT, 20 mM β-glycerophosphate, 0.5 mM PMSF, 60 μg/ml aprotinin, and 2 μg/ml leupeptin; incubated on ice for 15 min; and centrifuged at 10,000*g* at 4°C for 10 min. The resulting supernatant was assayed for protein concentrations. Twenty micrograms of protein extracts were incubated with 10 fmol of ^{32}P-labeled oligonucleotide probe for the AP-1 binding sequence as described elsewhere (Kim et al., 1998) at RT for 30 min in 20 μl of the binding buffer, consisting of 20 mmol/liter HEPES (pH 7.9), 0.2 mmol/liter EDTA, 0.2 mmol/liter EGTA, 80 mmol/liter NaCl, 0.3 mmol/liter $MgCl_2$, 1 mmol/liter DTT, 0.2 mmol/liter PMSF, 6% glycerol, and 2 μg polydeoxyinosinic-deoxycytidylic acid (Pharmacia, Piscataway, NJ) as a nonspecific competitor. For competition experiments, a mutant AP-1 oligonucleotide competitor as described by Kim et al. (1998) was also used. The DNA-protein complexes were electrophoresed on 4% nondenaturing polyacrylamide gels, and the gels were then dried, subjected to autoradiography, and analyzed with Scanning Image software (Molecular Dynamics, Sunnyvale, CA).

Behavior

Vestibuloocular and vestibulospinal reflexes are used as markers of the development of static vestibular compensation. In the present study, we chose frequency of horizontal spontaneous nystagmus as a marker, because it can be reliably measured with a video camera (Kitahara et al., 1995, 1997, 1998, 2002; Fukushima et al., 2001).

Eye movements were recorded with a Panasonic NV-M7 video camera with a zoom lens and replayed on a Mitsubishi E7 Black Diamond VCR and a Sony Trinitron color monitor. The frequency of UL-induced spontaneous nystagmus in animals with antisense probes (against c-fos or PPE mRNA), naloxone, and saline pretreatments into the ipsi-MVN was measured as the number of quick-phase beats occurring over periods of 15 sec (n = 8 in each group). Eye movements were replayed and counted three times for each animal and the means obtained. These measurements were made just before and 0.5, 1, 2, 4, and 6 hr after UL.

Statistical Analysis

Differences in data from two groups were examined by Student's *t*-test and among more than three groups by Scheffe's F-test. Statistical significances of changes after surgery were eval-

uated by repeated-measures ANOVA. $P < 0.05$ was considered significant.

RESULTS

PPE Expression in the MVN After UL and BL

There were few PPE-LIR neurons in the MVN of sham-operated animals (Fig. 1A). As a UL study, a substantial number of PPE-LIR neurons appeared in the ipsi-MVN by 6 hr with a maximum increase in number 1 day after UL (Fig. 1B) and then gradually disappeared 7 days after surgery (Fig. 1C). There were few UL-induced PPE-LIR neurons in any other central vestibular regions (data not shown).

As a BL study, PPE-LIR neurons in the MVN were observed 1 day after the second labyrinthectomy, because PPE expression shows a maximal increase 1 day after UL, as mentioned above. Simultaneous BL did not show any PPE expression in the MVN (Fig. 2A). More than a 7-day interval between the two-staged operations induced obvious PPE-LIR neurons in the MVN on the second operated side (Fig. 2B). In animals with a longer interval between the two stages, the number of second labyrinthectomy-induced PPE-LIR neurons in the ipsi-MVN was significantly increased (Fig. 2C).

PPE and Fos Expression in the MVN After UL and BL

After UL, Fos-LIR neurons were observed in several regions in the central vestibular system, as previously described (Kaufman et al., 1992; Cirelli et al., 1996; Darlington et al., 1996). We have focused on Fos expression mainly in the ipsi-MVN, with a maximal increase 6 hr after UL (Kitahara et al., 1995, 1997, 2002; Fukushima et al., 2001). In the present study, PPE-LIR neurons appeared in the ipsi-MVN by 6 hr, with a maximal increase in number 1 day after UL, as mentioned above. Therefore, we examined double-staining immunohistochemistry with PPE and Fos in samples from 9 hr postoperatively ($n = 2$). PPE-LIR was recognized mainly in cell somata and Fos-LIR in cell nuclei. Some of PPE-LIR neurons in the ipsi-MVN were also Fos immunopositive 9 hr after UL (Fig. 3A) and 9 hr after BL (a 14-day interval between two stages; Fig. 3B).

Western Blotting in Antisense Oligonucleotide Experiments

To check the appropriate antisense oligonucleotide probe injection site in the ipsi-MVN in each animal, we observed trypan blue in the transverse sections between the rostral (bregma: −10.50 mm) and caudal (bregma: −13.00 mm; Fig. 4) levels. Animals with inappropriate injection sites were excluded.

Postoperative 6 hr was selected as a time for Western blotting in the present study, because both Fos and PPE protein expressions in the ipsi-MVN were abundant and pCREB expression in the ipsi-MVN had not yet disappeared (Kim et al., 2000). Furthermore, pre-UL application of antisense probes into the ipsi-MVN could still be effective at that time (Ziolkowska et al., 1998).

Judged from results of Western blotting (Fig. 5), pre-UL application of the antisense against c-fos mRNA eliminated UL-induced nuclear Fos protein expression without any significant changes in nuclear pCREB expression, resulting in reduction of cytoplasmic PPE protein expression in the ipsi-MVN. Neither saline vehicle nor random oligonucleotide application had any significant effects on these protein expressions in the ipsi-MVN. Pre-UL application of the antisense against PPE mRNA eliminated UL-induced cytoplasmic PPE protein expression, without any significant changes in nuclear pCREB or Fos protein expression in the ipsi-MVN.

Gel Shift Assay in Antisense Oligonucleotide Experiments

Specificity of AP-1 DNA binding activity and changes in AP-1 DNA binding activity in the ipsi-MVN after UL are shown in Figure 6. The ipsi-MVN protein extracts, collected after sham operation (lane 1) and UL with preapplication of saline (lanes 2–6) or antisense probes into the ipsi-MVN (lanes 7–9), were incubated with ^{32}P-labeled AP-1 consensus oligonucleotide probe in the absence of unlabeled AP-1 oligonucleotide probe (–; lane 2) and in the presence of 10-fold (lane 3), 100-fold (lane 4), and 200-fold (lane 5) molar excesses of unlabeled AP-1 probe and 200-fold (lane 6) molar excess of unlabeled mutant AP-1 probe. Specificity of AP-1 DNA binding activity in the ipsi-MVN after UL was enhanced in lanes 2–6 ($*P < 0.05$). The AP-1 DNA binding activity was significantly increased by UL (lanes 1, 2; $*P < 0.05$) and decreased by pre-UL application of the antisense against c-fos mRNA (lanes 2, 7; $*P < 0.05$). Pre-UL application of the antisense against PPE mRNA or random oligonucleotide probes had no significant effects on the AP-1 DNA binding activity (lanes 2, 8, 9).

Vestibular Compensation in Antisense Oligonucleotide Experiments

Antisense oligonucleotide probes or naloxone applied into the MVN of sham-operated animals did not induce any static vestibular symptoms, such as barrel rotation, head tilt, or spontaneous nystagmus (data not shown). The results

Fig. 1. PPE expression in the ipsi-MVN after UL. **A:** There were few preproenkephalin (PPE)-like-immunoreactive (LIR) neurons in the medial vestibular nucleus (MVN) in sham-operated animals (sham). **B:** A substantial number of PPE-LIR neurons appeared in the ipsilateral MVN (ipsi-MVN), with a maximal increase in number 1 day after unilateral labyrinthectomy (UL1d). Arrowheads indicate typical PPE-LIR neurons. **C:** A substantial number of PPE-LIR neurons appeared in the ipsi-MVN by 6 hr, with a maximal increase in number 1 day after UL and then gradually disappeared 7 days after UL ($*P < 0.05$). Values are expressed as the mean number ± SE of PPE-LIR neurons in the ipsi-MVN for four animals. Scale bar = 20 μm.

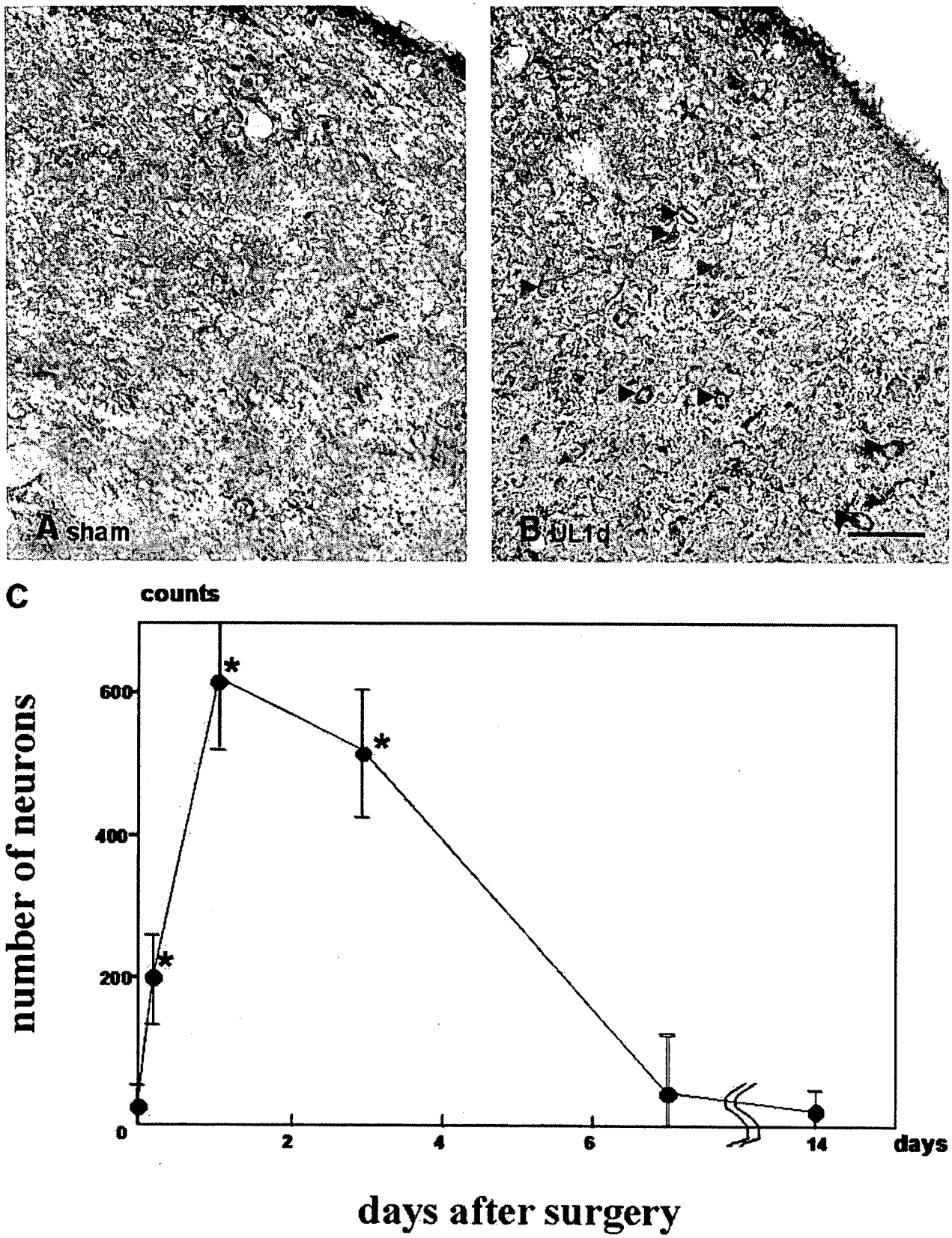
A sham
B UL1d
C
counts
number of neurons
600
400
200
0
2
4
6
14
days
days after surgery

Figure 1.

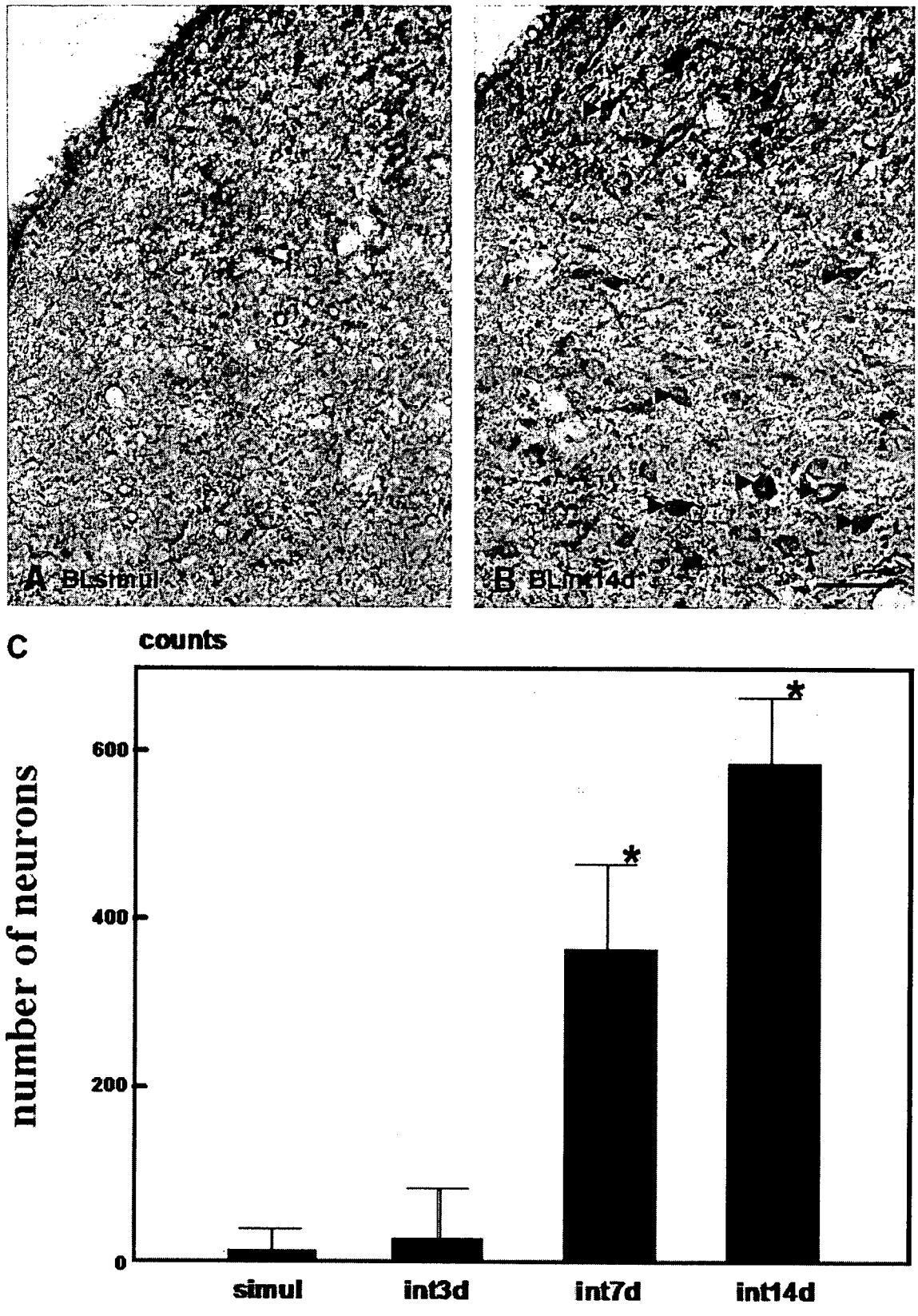
A BLsimul
B BLint14d
C
counts
number of neurons
600
400
200
0
*
*
simul
int3d
int7d
int14d

Figure 2.

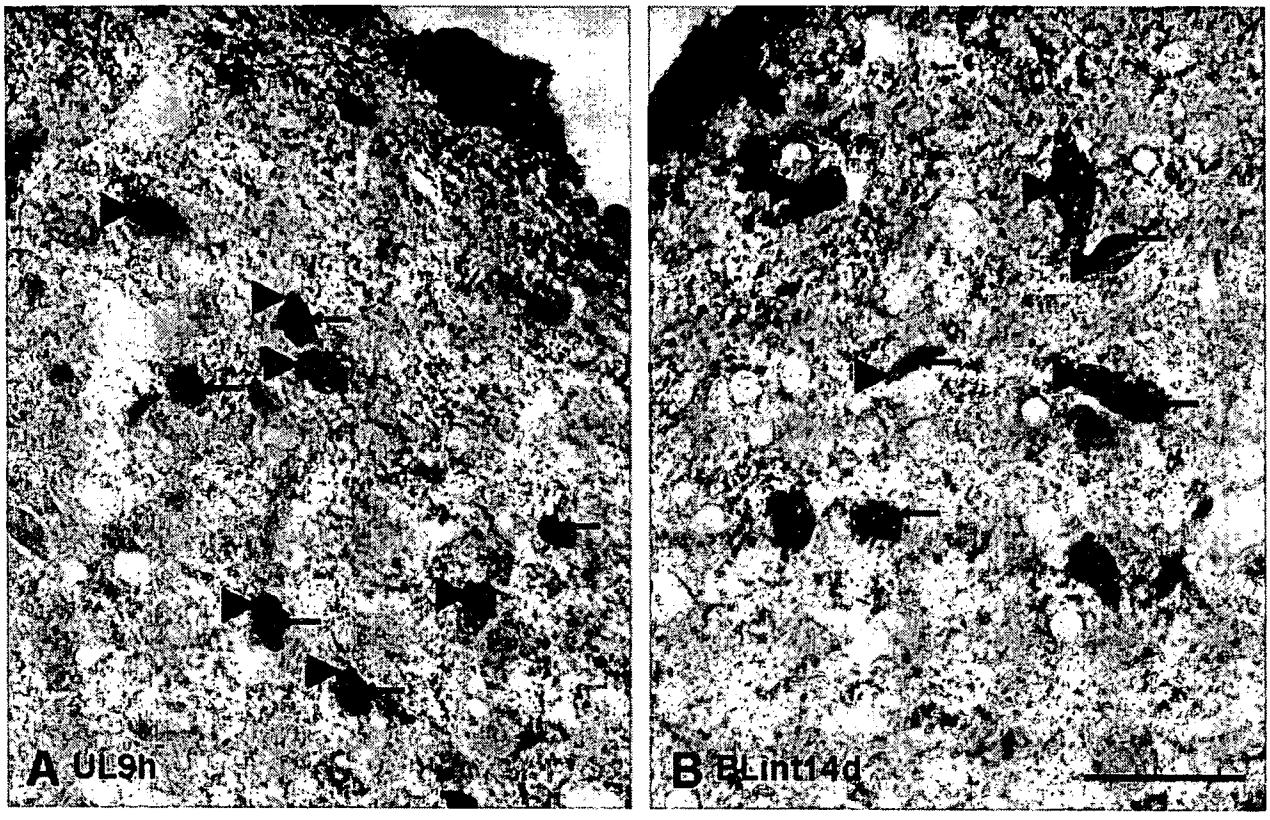

Fig. 3. PPE and Fos expression in the MVN after UL and BL. Higher magnification view of double-staining immunohistochemistry of preproenkephalin (PPE; arrowheads) and Fos (arrows) in the medial vestibular nucleus (MVN). PPE-like immunoreactivity (-LIR) was recognized in perikarya and Fos-LIR in cell nuclei. Some of PPE-LIR neurons were Fos-immunopositive 9 hr after unilateral labyrinthectomy (UL9h; **A**) and also 9 hr after bilateral labyrinthectomy (a 14-day interval between the two stages; BLint14d; **B**). Scale bar = 10 μm.

with c-fos antisense (Fig. 7B) suggested that depression of Fos-PPE signaling in the ipsi-MVN caused significantly more severe spontaneous nystagmus at the early stage and significantly more delay of vestibular compensation ($0.5 \leq h \leq 6$; $^{*}P < 0.05$). PPE antisense (Fig. 7C) and naloxone studies (Fig. 7D) both suggested that specific depression of enkephalinergic effects in the ipsi-MVN significantly delayed progress of vestibular compensation at the later stage ($4 \leq h \leq 6$; $^{**}P < 0.05$).

None of the four groups, A–D in Figure 7, showed any spontaneous nystagmus later than post-UL 48 hr, because static vestibular compensation in all these groups was accomplished around the same time after UL (data not shown). It was difficult to keep continuous the injection of antisense probes into the ipsi-MVN of alert animals using osmotic minipumps, even though this could be successfully performed just in the flocculus (Kitahara et al., 1998). Therefore, we took one-shot application of antisense probes in this study and plotted frequencies of spontaneous nystagmus in groups A–D just until 6 hr after UL (Fig. 7). One-shot application of antisense probes into the central nervous system could still be effective until that period (Ziolkowska et al., 1998), and it was consistent with Western blotting (Fig. 5).

Fig. 2. PPE expression in the MVN after BL. **A:** Simultaneous bilateral labyrinthectomy (BLsimul) induced few preproenkephalin (PPE)-like-immunoreactive (LIR) neurons in the medial vestibular nucleus (MVN) on the second operated side. **B:** A 14-day interval between two-staged operations (BLint14d) induced obvious PPE-LIR neurons in the MVN. Animals were sacrificed 1 day after the second labyrinthectomy. Arrowheads indicate typical PPE-LIR neurons. **C:** More than a 7-day interval between two-staged operations induced obvious PPE-LIR neurons in the MVN on the second operated side. In animals with a longer interval between the two operations, the number of second-labyrinthectomy-induced PPE-LIR neurons in the MVN was significantly increased ($^{*}P < 0.05$). Animals were sacrificed 1 day after the second labyrinthectomy. Values are expressed as the mean number ± SE of PPE-LIR neurons in the MVN for four animals. Simul, simultaneous bilateral labyrinthectomy; int3d, 3-day interval between two-staged operations; int7d, 7-day interval between the two; int14d, 14-day interval between the two. Scale bar = 20 μm.

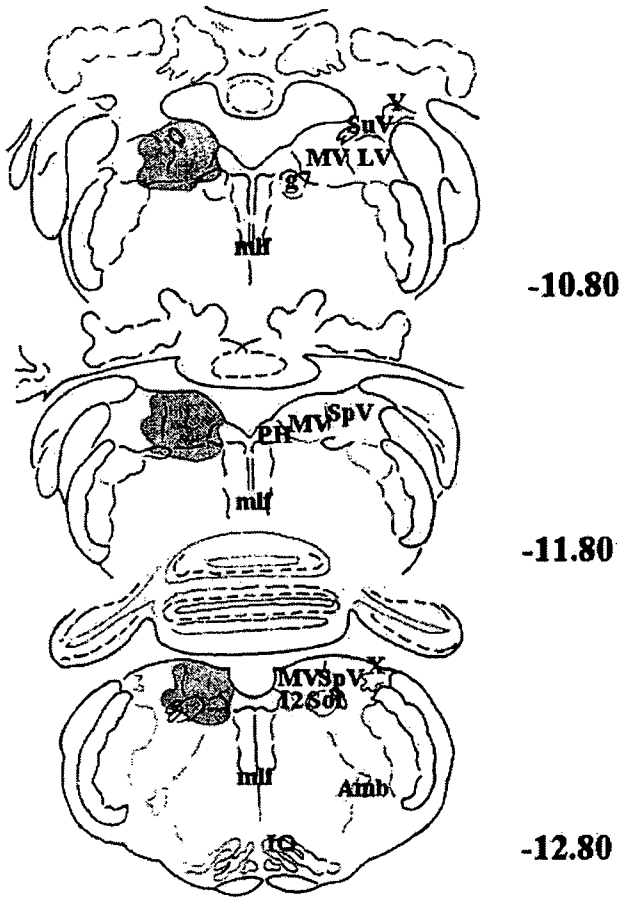

Fig. 4. Drawings of vestibular and vestibular-related nuclei in transverse sections illustrating injection sites of antisense oligonucleotide probes (As-f04). Three sections in the upper (bregma: −10.80 mm; **top**), middle (bregma: −11.80 mm; **middle**), and lower (bregma: −12.80 mm; **bottom**) levels are representative. 12, Hypoglossal nucleus; Amb, nucleus ambiguus; g7, genu of facial nerve root; IO, inferior olive; LV, lateral vestibular nucleus; mlf, med longitudinal fasciculus; MV, medial vestibular nucleus; PH, prepositus hypoglossal nucleus; Sol, solitary nucleus; SpV, spinal vestibular nucleus; SuV, superior vestibular nucleus; X, nucleus X; Y, nucleus Y.

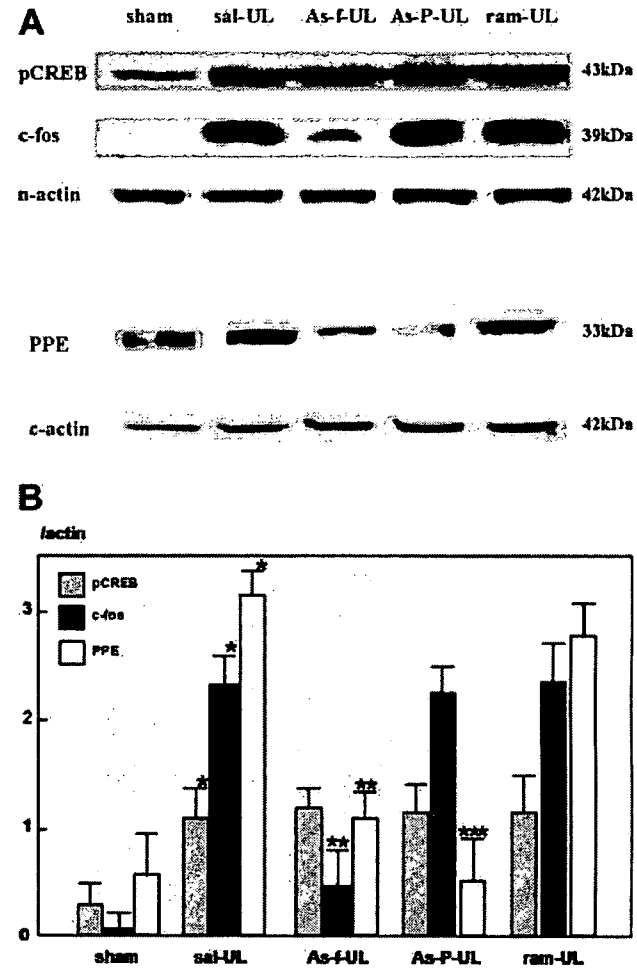

Fig. 5. Western blotting in antisense oligonucleotide experiments. **A:** Preunilateral labyrinthectomy (UL) application of antisense oligonucleotides had some effects on UL-induced protein expression in the ipsilateral medial vestibular nucleus (ipsi-MVN). **B:** All the data were also shown as intensity relative to nuclear β-actin expression for pCREB and Fos and cytoplasmic β-actin expression for PPE, respectively. $*P < 0.05$ between sham and sal-UL. $**P < 0.05$ between sal-UL and As-f-UL. $***P < 0.05$ among sal-UL, As-f-UL, and As-P-UL. Values are expressed as the mean intensity ± SE of each protein expression counted for four trials. pCREB, phosphorylated form of cAMP/calcium response element binding protein; c-fos, Fos protein; n-actin, nuclear β-actin; PPE, preproenkephalin protein; c-actin, cytoplasmic β-actin; sham, sham operated; sal-UL, pre-UL application of saline; As-f-UL, pre-UL application of antisense against c-fos mRNA; As-P-UL, pre-UL application of antisense against PPE mRNA; ram-UL, pre-UL application of random oligonucleotides.

DISCUSSION

In the present study, we first observed up-regulation in PPE-LIR in the ipsi-MVN after UL. By means of double-staining immunohistochemistry with PPE and Fos, we revealed that some of these PPE-LIR neurons were also Fos immunopositive. The time course of decay of these double-stained neurons in the ipsi-MVN was quite parallel with that of the UL-induced behavioral deficits, as previously reported (Kitahara et al., 1995, 1997, 1998; Fukushima et al., 2001). Fos is usually used as a marker of neuronal activation (Lee and Beitz, 1993) and possibly regulates PPE mRNA expression, because the PPE gene has a DNA binding site (AP-1) in its promoter region (Sonnenberg et al., 1989). Therefore, these findings suggest that, after UL, some of the ipsi-MVN neurons could be activated and start PPE expression, resulting in vestibular compensation.

When two labyrinths are successively destroyed, a reversal of the direction of asymmetry is observed following the second labyrinthectomy (Bechterew's phenomenon), if vestibular compensation for the first labyrinthectomy has already taken place (Galiana et al., 1984). We next examined relationships between this phenom-

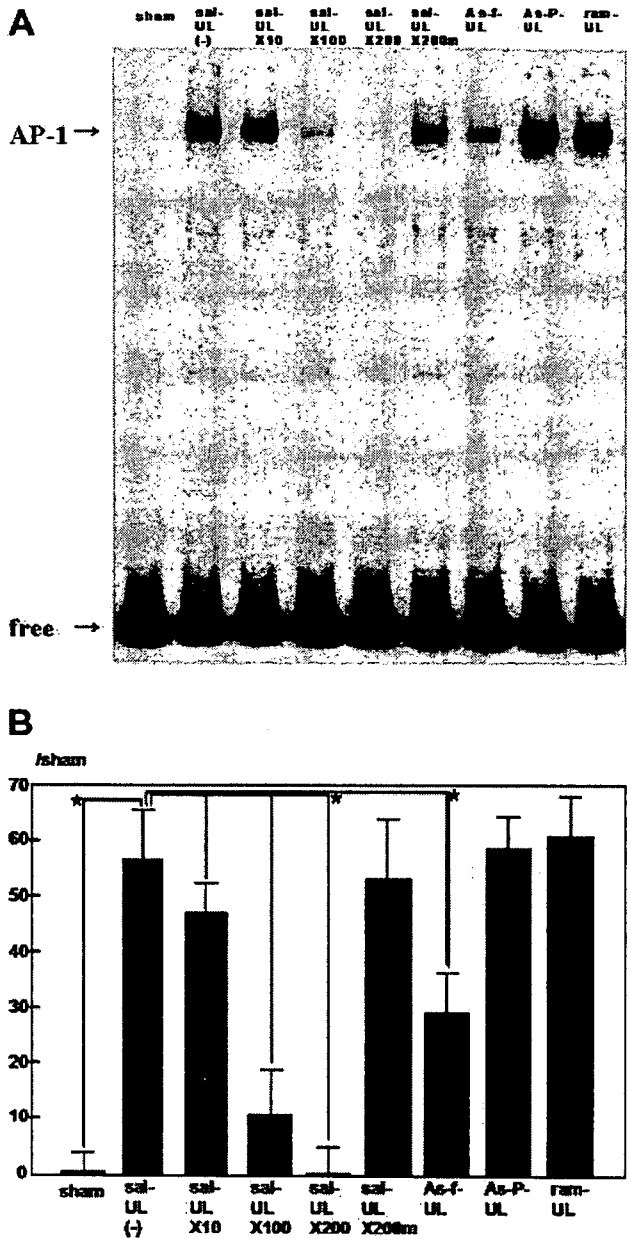

Fig. 6. Gel shift assay in antisense oligonucleotide experiments. **A:** Protein extracts in the ipsilateral medial vestibular nucleus (ipsi-MVN) after sham operation (sham) were collected (lane 1). Those after unilateral labyrinthectomy with preapplication of saline (sal-UL; lanes 2–6) or antisense probes (As-UL; lanes 7–9) were also collected. All samples were incubated with ^{32}P-labeled AP-1 consensus oligonucleotide probe in the absence of unlabeled AP-1 oligonucleotide probe (–; lane 2) and in the presence of 10-fold (×10; lane 3), 100-fold (×100; lane 4), and 200-fold (×200; lane 5) molar excess of unlabeled AP-1 probe and 200-fold molar excess of unlabeled mutant AP-1 probe (×200m; lane 6). **B:** All the data are also shown as intensity relative to that in lane 1. $*P < 0.05$ between samples. Values are expressed as the mean intensity ± SE of each AP-1 DNA binding activity counted for four trials.

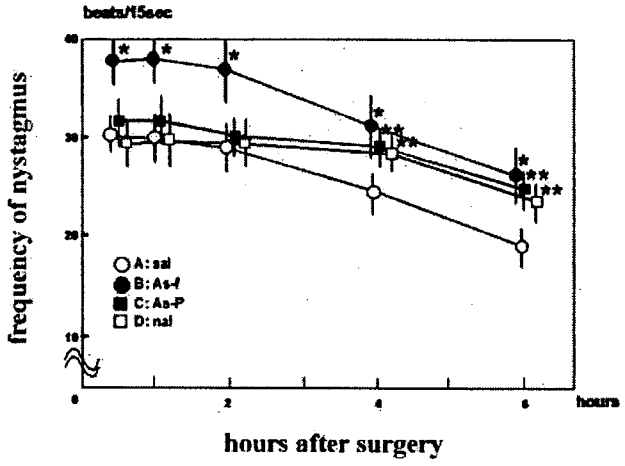

Fig. 7. Vestibular compensation in antisense oligonucleotide experiments. Preunilateral labyrinthectomy (UL) application of c-fos antisense caused significantly much more severe spontaneous nystagmus at the early stage and significantly much more delay in vestibular compensation ($0.5 \leq h \leq 6$; $*P < 0.05$). Pre-UL application of preproenkephalin (PPE) antisense and naloxone both demonstrated significantly much more delay in vestibular compensation ($4 \leq h \leq 6$; $**P < 0.05$). Values are expressed as the mean frequency ± SE of quick phase beats per 15 sec for eight animals. Sal, pre-UL application of saline; As-f, pre-UL application of antisense against c-fos mRNA; As-P, pre-UL application of antisense against PPE mRNA; nal, pre-UL application of naloxone.

enon and PPE -LIR in the MVN after two-staged BL. An interval of >1 week between the two stages induced up-regulation of PPE-LIR on the second operated side, although this was never seen with an interval of <1 week. In addition, an interval of >1 week between the two stages led to Bechterew's phenomenon, although never in the case of an interval of <1 week (Saika et al., 1993; Kitahara et al., 2002). Therefore, these findings suggest that changes in PPE expression in the MVN could be involved in behavioral performances not only after UL but after two-stage BL.

In the present study, some of PPE-LIR neurons were also Fos immunopositive after BL. However, in our previous study, an interval of at least 6 hr between the two stages could induce up-regulation of Fos-LIR in the MVN on the second operated side, unlike PPE-LIR (Kitahara et al., 2002). This discrepancy may be due to the fact that only a part of these Fos-LIR neurons could regulate PPE expression in the ipsi-MVN after UL and BL. Actually, these Fos-LIR neurons, which were induced after BL with an interval of 6 hr to 1 week between the two stages, mainly projected their axons into the vestibulocerebellum (Kitahara et al., 2002) and might not be related to consequent PPE expression.

Double staining with Fos and PPE in the ipsi-MVN cannot, by itself, prove that Fos regulates PPE expression in the ipsi-MVN. However, the gel shift assay and Western blotting revealed that elimination of Fos expression significantly reduced both AP-1 DNA binding activity and

PPE expression in the ipsi-MVN after UL. These results indicate that UL-induced Fos expression in the ipsi-MVN enhances AP-1 activity and up-regulates PPE expression. A partner of Fos is necessary to bind and activate AP-1 in promoting expression of some genes. Although changes in expression of other immediate early genes after UL have been reported (Darlington et al., 1996), the partner of Fos has not been clarified yet. With regard to the intracellular signaling, pCREB is a transcription factor for immediate early genes, including Fos, and it is actually up-regulated in the bilateral MVN at the early stage after UL (Kim et al., 2000). Western blotting also confirmed the up-regulation of pCREB in the ipsi-MVN after UL in the present study. Therefore, there is a possibility that pCREB-Fos-PPE signaling in the ipsi-MVN could be enhanced after UL.

Fos-PPE signal modulation in the MVN during vestibular compensation was clearly demonstrated in the present study. To determine whether the modulation is for or against vestibular compensation, we checked the amount of spontaneous nystagmus until 6 hr postoperatively with pre-UL application of antisense probes. C-fos antisense study revealed that depression of Fos-PPE signaling in the ipsi-MVN caused significantly more severe behavioral deficits at the very early stage just after UL and significantly more delay of vestibular compensation at the chronic stage around 6 hr after UL. Behavioral deficits at the very early stage just after UL come from imbalance between bilateral MVN activities, which is partially compensated through the vestibular commissure and/or vestibulocerebellar inhibition on the contralateral side. Without contralateral inhibition, much more severe vestibular imbalance occurred immediately after UL (McCabe and Ryu, 1969; Kitahara et al., 1997). Therefore, much more severe behavioral deficits at the very early stage just after UL in c-fos antisense-treated animals indicate that UL-induced Fos expression in the ipsi-MVN has an important role in rebalancing between bilateral MVN activities via commissure and/or vestibulocerebellum. However, PPE antisense and naloxone antagonist studies both demonstrated that specific depression of enkephalinergic effects in the ipsi-MVN did not have an effect at the very early stage just after UL but caused significantly more delay of vestibular compensation at the chronic stage around 6 hr after UL. These results, taken together with those in the c-fos antisense study, indicate that Fos-PPE signaling in the ipsi-MVN could be effective mainly at the chronic stage rather than at the very early stage.

What is the significance of Fos-PPE signaling in the ipsi-MVN at the chronic stage of vestibular compensation? The regeneration of the resting activity in the ipsi-MVN type I neurons, which receive primary afferent inputs, becomes more important for the restoration of balance between bilateral MVN activities at the later chronic stage (Kitahara et al., 1998). According to previous reports, whereas opiates directly activate 30% of the MVN neurons via μ- and/or δ-opioid receptors (Lin and Carpenter, 1994), only δ-opioid receptors demonstrate inhibitory effects on most of the MVN neurons (Sulaiman and Dutia, 1998). These two different reports could prepare the way for two different kinds of explanation for opioid receptor-mediated recovery of the ipsi-MVN type I neuronal activities after UL. UL-induced Fos-PPE signaling in some of the ipsi-MVN neurons that are not type I but vestibular interneurons might activate the MVN type I neurons via the opioid receptor activation (if the opioid receptor activates the MVN, as in Fig. 8A) or inactivate inhibitory interneurons via the opioid receptor activation to disinhibit the MVN type I neurons (if the opioid receptor inhibits the MVN, as in Fig. 8B). The restoration of balance between intervestibular nuclear activities, thereafter, could also correct the oculomotor asymmetry via vestibuloocular neurotransmission at the chronic stage. However, in previous reports, no protein production was required (Ris et al., 1998), and intrinsic pacemaker-like excitability was important (Him and Dutia, 2001) for recovery of the resting activity in the ipsi-MVN type I neurons after UL. Actually, even after simultaneous BL, the resting activity in the MVN can finally return to the normal level (Ris and Godaux, 1998). Therefore, Fos-PPE signaling might not be indispensable for recovery of the resting activity in the ipsi-MVN type I neurons after UL, but the signaling could contribute to facilitation of the recovery, resulting in progress of vestibular compensation.

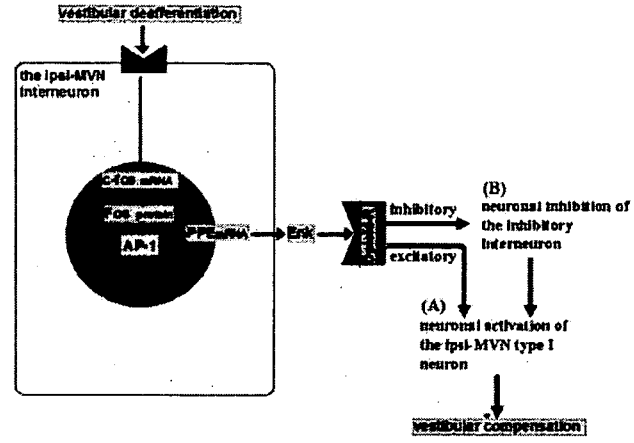

Fig. 8. Schematic representation of the relationship between Fos-PPE signaling and vestibular compensation. Immediately after unilateral vestibular deafferentiation, Fos is induced in some of the ipsilateral medial vestibular nucleus (ipsi-MVN) interneurons, probably via disinhibitory mechanisms. Some of these Fos-contained neurons could regulate preproenkephalin (PPE) and enkephalin (Enk) expression via the AP-1 activation and facilitate the restoration of the ipsi-MVN type I neuronal activities via the opioid receptor (opioid-R) activation (directly in A or indirectly in B), resulting in progress of vestibular compensation.

In conclusion, immediately after a great loss of unilateral vestibular periphery, Fos is induced in some of the ipsi-MVN interneurons. Some of these Fos-contained neurons could regulate consequent PPE expression via the AP-1 activation and facilitate the restoration of balance between bilateral MVN type I activities via opioid receptor activation, contributing to the development of vestibular compensation.

ACKNOWLEDGMENTS

We thank Prof. Carey D. Balaban (Department of Otolaryngology, University of Pittsburgh School of Medicine) and Prof. Hiroshi Kiyama (Department of Neuroanatomy, Osaka City University School of Medicine) for helpful advice and support.

REFERENCES

Aldrich EM, Peusner KD. 2002. Vestibular compensation after ganglionectomy: ultrastructural study of the tangential vestibular nucleus and behavioral study of the hatchling chick. J Neurosci Res 67:122–138.

Cirelli C, Pompeiano M, D'Ascanio P, Arrighi P, Pompeiano O. 1996. C-fos expession in the rat brain after unilateral labyrinthectomy and its relation to the uncompensated and compensated stages. Neuroscience 70:515–546.

Darlington CL, Lawlor P, Smith PF, Dragunow M. 1996. Temporal relationship between the expression of fos, jun and krox-24 in the guinea pig vestibular nuclei during the development of vestibular compensation for unilateral vestibular deafferentation. Brain Res 735:173–176.

Delogni P, Niman H, Raymond V, Sawchenko P, Verma IM. 1988. Detection of fos protein during osteogenesis by monoclonal antibodies. Mol Cell Biol 8:2251–2256.

Dutia MD, Gilchrist DPD, Sansom AJ, Smith PF, Darlington CL. 1996. The opioid receptor antagonist, naloxone, enhances ocular motor compensation in guinea pig following peripheral vestibular deafferentiation. Exp Neurol 141:141–144.

Fukushima M, Kitahara T, Takeda N, Saika T, Uno A, Kubo T. 2001. Role of cholinergic mossy fibers in medial vestibular and prepositus hypoglossal nuclei in vestibular compensation. Neuroscience 102:159–166.

Galiana HL, Flohr H, Melvill Jones G. 1984. A reevaluation of intervestibular nuclear coupling: Its role in vestibular compensation. J Neurophysiol 51:242–259.

Goto MM, Romero GG, Balaban CD. 1997. Transient changes in flocculonodular lobe protein kinase C expression during vestibular compensation. J Neurosci 17:4367–4381.

Gundersen HJG. 1978. Estimation of the number of objects per area unbiased by edge effects. Microsc Acta 81:107–117.

Him A, Dutia MB. 2001. Intrinsic excitability changes in vestibular nucleus neurons after unilateral deafferentation. Brain Res 908:58–66.

Kaufman GD, Anderson JH, Beitz AJ. 1992. Brainstem Fos expression following acute unilateral labyrinthectomy in the rat. Neuroreport 3: 829–832.

Kaufman GD, Shinder ME, Perachio AA. 1999. Correlation of Fos expression and circling asymmetry during gerbil vestibular compensation. Brain Res 817:246–255.

Kim MS, Kim JH, Lee MY, Chun SW, Lee SH, Park BR. 2000. Identification of phospholylated form of cAMP/calcium responsive element binding protein expression in the brain stem nuclei at early stage of vestibular compensation in rats. Nurosci Lett 290:173–176.

Kim S, Izumi Y, Yano M, Hamaguchi A, Miura K, Yamanaka S, Miyazaki H, Iwao H. 1998. Angiotensin blockade inhibits activation of mitogen-activated protein kinases in rat balloon-injured artery. Circulation 97:1731–1737.

Kitahara T, Takeda N, Saika T, Kubo T, Kiyama H. 1995. Effects of MK801 on Fos expression in the rat brainstem after unilateral labyrinthectomy, Brain Res 700:182–190.

Kitahara T, Takeda N, Kubo T, Kiyama H. 1997. Role of the flocculus in the development of vestibular compensation: immunohistochemical studies with retrograde tracing and flocculectomy using Fos expression as a marker in the rat brainstem. Neuroscience 76:571–580.

Kitahara T, Takeda N, Kubo T, Kiyama H. 1998. An implication of protein phosphatase 2A-β in the rat flocculus for lesion-induced vestibular plasticity. Acta Otolaryngol 118:685–691.

Kitahara T, Nakagawa A, Fukushima M, Horii A, Takeda N, Kubo T. 2002. Changes in Fos expression in the rat brainstem after bilateral labyrinthectomy. Acta Otolaryngol 122:620–626.

Lee JH, Beitz AJ. 1993. The distribution of brain stem and spinal cord nuclei associated with different frequencies of electroacupuncture analgesia. Pain 52:11–28.

Lee T, Kaneko T, Taki K, Mizuno N. 1997. Preprodynorphin-, preproenkephalin- and preprotachykinin-expressing neurons in the rat neostriatum: an analysis by immunocytochemistry and retrograde tracing. J Comp Neurol 386:229–244.

Lin Y, Carpenter DO. 1994. Direct excitatory opiate effects mediated by non-synaptic actions on rat medial vestibular neurons. Eur J Pharmacol 262:99–106.

Llinas R, Walton K. 1979. Vestibular compensation: a distributed property of the central nervous system. In: Asanuma H, Wilson VJ, editors. Integration in the nervous system. Tokyo: Igaku Shoin. p 145–166.

McCabe BF, Ryu JH. 1969. Experiments of vestibular compensation. Laryngoscope 79:1728–1736.

Nicot A, Ogawa S, Berman Y, Carr KD, Pfaff DW. 1997. Effects of an intrahypothalamic injection of antisense oligonucleotides for preproenkephalin mRNA in female rats: evidence for opioid involvement in lordosis reflex. Brain Res 777:60–68.

Paxinos G, Watson C. 1986. The rat brain in stereotaxic coordinates. New York: Academic Press.

Precht W, Dieringer N. 1985. Neuronal events paralleling functional recovery (compensation) following peripheral vestibular lesions. In: Berthoz A, Melvill Jones G, editors. Adaptive mechanism in gaze control, facts and theories. Amsterdam: Elsevier. p 251–268.

Ris L, Godaux E. 1998. Neuronal activity in the vestibular nuclei after contralateral or bilateral labyrinthectomy in the alert guinea pig. J Neurophysiol 80:2352–2367.

Ris L, Wattiez R, de Waele C, Vidal PP, Godaux E. 1998. Reappearance of activity in the vestibular neurons of labyrinthectomized guinea pigs is not delayed by cycloheximide. J Physiol 512:533–541.

Saika T, Takeda N, Kiyama H, Kubo T, Tohyama M, Matsunaga T. 1993. Changes in preproenkephalin mRNA after unilateral and bilateral labyrinthetomy in the rat medial vestibular nucleus. Brain Res Mol Brain Res 19:237–240.

Sonnenberg JL, Rauscher IIIFJ, Morgan JI, Curran T. 1989. Regulation of proenkephalin by Fos and Jun. Science 246:1622–1625.

Sulaiman MR, Dutia MB. 1998. Opioid inhibition of rat medial vestibular nucleus neurones in vitro and its dependence on age. Exp Brain Res 122:196–202.

Tokuyama S, Zhu H, Oh S, Ho IK, Yamamoto T. 2001. Further evidence for a role of NMDA receptors in the locus coeruleus in the expression of withdrawal syndrome from opioids. Neurochem Int 39:103–109.

Ziolkowska B, Przewlocka B, Mika J, Labuz D, Przewlocki R. 1998. Evidence for Fos involvement in the regulation of proenkephalin and prodynorphin gene expression in the rat hippocampus. Brain Res Mol Brain Res 54:243–251.

Otology & Neurotology
27:896–900 © 2006, Otology & Neurotology, Inc.

Factors Relating to the Vertigo Control and Hearing Changes Following Intratympanic Gentamicin for Intractable Ménière's Disease

Arata Horii, Takanori Saika, Atsuhiko Uno, Suetaka Nishiike, Kenji Mitani, Masato Nishimura, Tadashi Kitahara, Munehisa Fukushima, Aya Nakagawa, Chisako Masumura, Tomo Sasaki, Kaoru Kizawa, and Takeshi Kubo

Department of Otolaryngology, Osaka University Medical School, Japan

Objective: To look for factors relating to the vertigo control and hearing changes after intratympanic injections of gentamicin (GM).
Study design: Prospective.
Setting: Tertiary referral medical center.
Patients: Twenty-eight patients with intractable Ménière's disease.
Interventions: Three intratympanic injections of GM (once per day for three consecutive days).
Main Outcome Measures: Although five patients needed further GM injections or vestibular neurectomy because of poor control (Group I), 23 patients had their vertigo controlled for more than two years without further treatment (Group II). The number of vertigo spells per month, pure-tone audiometry, electrocochleography, caloric response, post-head shake nystagmus, and plasma vasopressin as a stress marker were examined.
Results: Before GM injections, there was no difference in the number of vertigo spells per month between Groups I and II. However, the hearing thresholds were higher in Group I. Hearing improvement, increase in percentage of canal paresis and induction of post-head shake nystagmus were observed after GM injections only in Group II. Even in the 11 patients who showed an improvement in hearing of more than 10 dB (hearing improvement group), percentage of canal paresis was increased after GM. More, premedication plasma vasopressin levels were lower in the hearing improvement group as compared with the hearing loss/no changes group. Four of eight patients became negative for dominant negative summating potential in electrocochleography after GM injections in the hearing improvement group.
Conclusion: Our data indicate that the frequency of vertigo is not a key factor in the vertigo control after GM injections, that induction of vestibular damage in the injected ear is essential for the control of vertigo and this effect is mostly pronounced in patients with milder hearing loss, and that hearing improvement is not only a consequence of good vertigo control but also affected by the stress level before treatment. **Key Words:** Caloric response—Electrocochleography—Gentamicin—Hearing—Ménière's disease—Post-head shake nystagmus— Vasopressin.
Otol Neurotol **27**:896–900, 2006.

Most patients with Ménière's disease can be effectively treated by medical means including a low-salt diet, diuretics, steroids, vasodilators, calcium channel blockers, and other agents (1). For medically intractable Ménière's disease, various surgical techniques including vestibular neurectomy, endolymphatic sac surgery, and labyrinthectomy have been performed. However, endolymphatic sac surgery is criticized because of its poor results with respect to long-term vertigo control (2), whereas labyrinthectomy damages the cochlear function.

Address correspondence and reprint requests to Arata Horii, M.D., Ph.D., Department of Otolaryngology, Osaka University Medical School, 2-2 Yamadaoka, Suita, Osaka 565-0871, Japan; E-mail:ahorii@ent.med.osaka-u.ac.jp.

This study was partly supported by a Research Grant for Intractable Disease (Vestibular Disorders) from the Ministry for Health and Welfare of Japan.

Recently, intratympanic injections of gentamicin (GM) have gained popularity so as to replace vestibular surgery for intractable Ménière's disease. In fact, various protocols have recently reported excellent control of vertigo spells and minimum damage to cochlear function (3–8). However, some patients actually do not respond to this treatment, and surgical interventions are advocated. In this prospective study, we treated 28 patients with intractable Ménière's disease by three intratympanic injections of GM. The aim of this study was to clarify the factors relating to vertigo control and hearing changes after intratympanic GM. Various data were compared between patients who were followed for more than two years without additional treatments and those who had to receive additional GM injections or vestibular neurectomy because of the poor vertigo control.

The following data were compared: vertigo spells per month, hearing levels and electrocochleography (EcochG)

as markers for cochlear function, caloric response and post-head shake nystagmus (post-HSN) as markers for vestibular function, and plasma vasopressin (AVP) level as a stress marker (9).

MATERIALS AND METHODS

This study was conducted under the guidelines approved by the ethical committee of Osaka University Hospital.

Twenty-eight patients with unilateral Ménière's disease were treated by intratympanic GM. Their ages ranged from 26 to 71 years (mean ± SD, 51.4 ± 12.2 years), and the sex ratio was 9 men and 19 women. Their conditions had been present for at least six months and had not been cured by any medical treatment. Before undergoing GM injections, patients were treated with 90 ml of isosorbide (diuretics) and 75 mg of diphenidol (antivertigo drugs) per day and injected with 200 ml of glycerol when indicated. Some patients were also prescribed a minor tranquilizer.

After hospital admission, patients received one GM injection per day for three consecutive days as follows: 0.4 to 0.6 ml of GM (26.7 mg/ml in buffered solution) was administered transtympanically to patients using a 23-gauge needle under an operating microscope in supine position, in which they were advised to stay for 30 minutes after injections. No water irrigation was performed after GM injections.

Of the 28 patients, 4 received additional GM injections, and 1 underwent vestibular neurectomy because of poor vertigo control. The other 23 had their vertigo well controlled for more than two years without further GM injections or surgery. The former 5 patients were classified as Group I, whereas the latter 23 patients were classified as Group II. The follow-up period for Group II was 24 to 54 months (mean ± SD, 35.7 ± 10.0 months). Group I patients received additional GM injections 3, 4, 7, and 28 months after the initial GM treatment. One patient underwent vestibular neurectomy 14 months after the GM treatment. Of the five Group I patients, one had a chronic otitis media, which made the GM perfusion through the round window less effective. Additional intratympanic GM to the Group I patients induced a progression (mean ± SE) of percentage of canal paresis (CP%) to 76.0 ± 12.4% and an appearance of post-HSN, resulting in the control of vertigo spells.

Examinations performed in this study included pure-tone audiogram (PTA), EcochG, bithermal caloric testing, post-HSN, and measurements of plasma AVP levels. Other examinations such as magnetic resonance imaging of the brain and posturography were also performed if indicated.

EcochG was recorded from the external auditory canal using a Neuropack 2 equipment (Nihon Kohden, Tokyo, Japan), and the negative summating potential (−SP)-to-action potential ratio was obtained and used as a sign for endolymphatic hydrops. Based on the previously measured baseline of our department, a negative SP-to-action potential ratio of more than 0.4 was regarded as a significant sign of "dominant −SP", suggesting endolymphatic hydrops. The vestibular function was assessed by caloric testing, and the CP% was calculated using Jongkees formula. Accordingly, CP% was defined as an interear difference of maximum slow phase eye velocity as expressed in the usual electronystagmography report. Electronystagmography was recorded using an EN1100 model (NEC, Tokyo, Japan) with a 3-second time constant in alternating current mode. Accordingly, 0% indicated an absence of right-to-left difference, whereas 100% was indicative of a total canal paresis. In our department, abnormal right-to-left difference is considered when CP% is 21% or greater. Because plasma AVP levels have a diurnal secretion pattern, they were measured in the morning in all patients. For Group II, all these examinations were performed just before and 6 to 12 months after GM injections. For Group I, they were measured just before the additional treatments and before the initial GM.

The treatment outcome on hearing and equilibrium was basically evaluated following the American Academy of Otolaryngology–Head and Neck Surgery guidelines (10): the frequency of definitive attacks for the period of six months before treatment should be compared with the interval between 18 and 24 months after treatment, hearing comparison (0.5, 1, 2, and 3 kHz) should be made with the worst audiogram of each of the two six-month intervals, and 10 dB or more changes in hearing were considered significant. However, threshold levels of 3 kHz are not usually measured in Japan. Therefore, we adopted the average hearing thresholds of 0.25, 0.5, 1, and 2 kHz. In Group I, the worst audiogram between the initial GM and the additional treatments was used as the post-GM hearing level.

Differences in the results of various examinations between the pre- and post-GM periods and the treatment outcome were tested using the Wilcoxon signed-rank test (vertigo spells, hearing levels, CP%, and plasma AVP). Differences between groups (Group I versus Group II, hearing improvement versus hearing loss/no changes) were tested using the Mann-Whitney U test (hearing levels and plasma AVP) or Chi square test (post-HSN and dominant −SP). p values < 0.05 were considered significant.

RESULTS

Vertigo Spells

Figure 1 shows the number of vertigo spells per month. In Group II, the number of vertigo spells between 18 and 24 months after GM injections was significantly lower than that in the six-month period before treatment

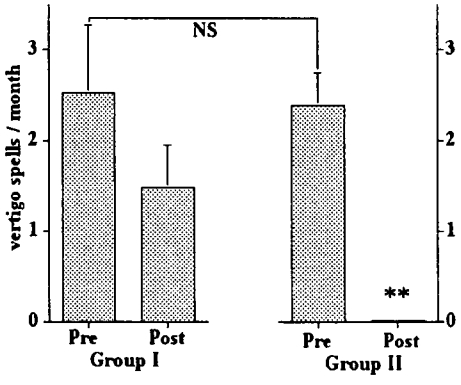

FIG. 1. Vertigo spells per month before and after GM injections. Left: Number of vertigo spells per month during six months before intratympanic GM injections (pre) and that between the initial GM and additional treatments (post) of Group I. Right: Number of vertigo spells per month during 6 months before intratympanic GM injections (pre) and that between 18 and 24 months after treatment (post) of Group II. No difference in vertigo spells was noted before GM injections between Groups I and II. In Group II, the number of vertigo spells was lower during the post-GM period than during the pre-GM one ($p < 0.0001$).

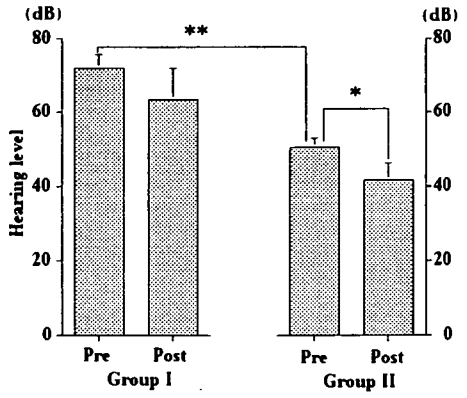

FIG. 2. Hearing levels before and after GM injections. The worst threshold level during the six-month periods just before intratympanic GM injections (pre) and that between the initial GM injection and additional treatments (post) is shown for Group I. The worst threshold level during the six-month periods just before intratympanic GM injections (pre) and that between 18 and 24 months after treatment (post) is shown for Group II. Hearing threshold before GM was lower in Group II as compared with that in Group I ($p = 0.0033$). In Group II, hearing thresholds were lower in the post-GM period as compared with those in the pre-GM one ($p = 0.0401$).

($p < 0.0001$); there was no difference in the number of vertigo spells between the pre- and post-GM periods in Group I. In addition, no difference in the number of vertigo spells at pre-GM was noted between Groups I and II.

Hearing

Hearing levels improvement (mean ± SE) from 50.4 ± 2.7 to 41.9 ± 4.4 dB after GM injections was recorded in Group II (Fig. 2, $p = 0.0401$); there was no difference in the hearing levels between the pre- and post-GM periods in Group I. As shown in Figure 2, pre-GM hearing in Group II (50.4 ± 2.7 dB) was significantly better than that in Group I (72.0 ± 3.5 dB) ($p = 0.0033$).

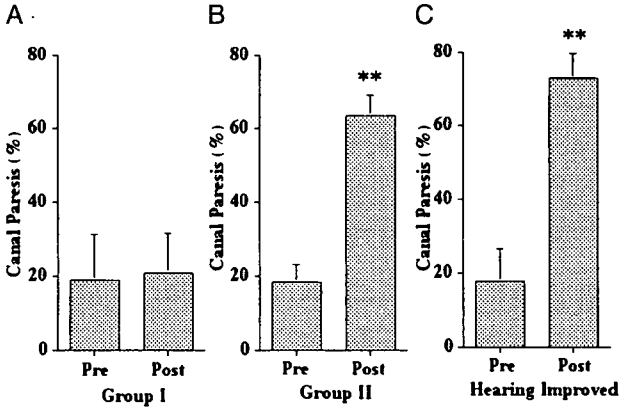

FIG. 3. Percentage of canal paresis before and after GM injections. The CP% measured at pre- and post-GM in Group I (Fig. 3*A*), Group II (Fig. 3*B*), and the hearing improvement group (Fig. 3*C*) are shown. Intratympanic GM injections significantly increased CP% in Group II ($p < 0.0001$) but not in Group I. Even in the hearing improvement group, CP% was significantly increased after the GM treatment ($p = 0.0051$).

TABLE 1. *Post-head shake nystagmus by group*

	Post-HSN (+)	
	Pre-GM	Post-GM
Group I	0/5	1/5
Group II	5/22	20/23[a]

A/B: "A" is the number of patients with post-HSN, whereas "B" is the number of patients examined.
GM indicates gentamicin; HSN, post-head shake nystagmus.
[a] $p < 0.0001$ versus pre-GM.

Canal Paresis and Post-HSN

Although there was no difference in CP% between the pre- and post-GM periods in Group I (Fig. 3A), CP% (mean ± SE) was significantly increased from 18.2 ± 4.9 to 63.5 ± 5.6% after GM injections in Group II (Fig. 3B, $p < 0.0001$). Table 1 shows the effects of intratympanic GM on the induction of post-HSN. Intratympanic GM significantly induced a post-HSN beating to the opposite side from the injected ear only in Group II ($p < 0.0001$). As shown in the Hearing Changes section, under Results, there were 11 patients whose hearing was improved by more than 10 dB (hearing improvement group). Even in this hearing improvement group, CP % was significantly increased after GM injections ($p = 0.0051$, Fig. 3C).

Plasma AVP

As shown in Figure 4B, plasma AVP levels decreased after GM injections in Group II ($p = 0.04$); there was no difference between the pre- and post-GM periods in Group I (Fig. 4A).

Hearing Changes

In this study, data of patients with reduced hearing were combined with those without hearing changes: hearing

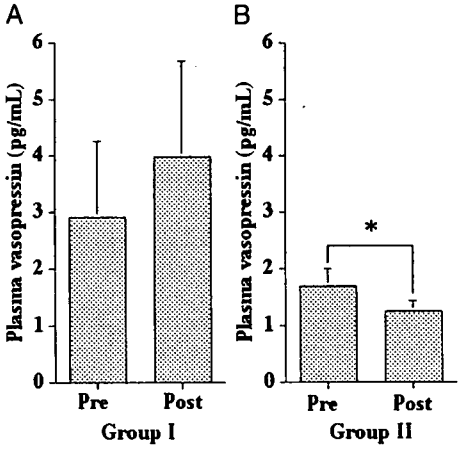

FIG. 4. Plasma AVP levels before and after GM injections. Plasma AVP levels decreased after GM injections only in Group II (Fig. 4*B*, $p = 0.04$) but not in Group I (Fig. 4*A*).

TABLE 2. *Factors relating to hearing changes after gentamicin injections*

	Hearing	
	Loss/No Changes	Improvement
No. of Patients	17	11
Pre-PTA (dB)	55.4 ± 3.5	52.4 ± 4.7
EcochG: (+) → (−)	0/7	4/8[a]
Pre-AVP (pg/ml)	2.31 ± 0.51	1.02 ± 0.22[a]

Hearing loss means that PTA (post) shows a decrease of more than 10 dB as compared with those in the pretreatment one, whereas hearing improvement means an improvement of more than 10 dB. EcochG (+) → (−) means that dominant −SP disappeared after GM. A/B: "A" is the number of patients who had dominant −SP but lost it after GM, whereas "B" is the number of patients who had dominant −SP before GM.

[a] $p < 0.05$ versus loss/no changes.

AVP indicates vasopressin; EcochG, electrocochleography; GM, Gentamicin; PTA, pure-tone audiogram.

loss/no changes group. There were 11 patients who showed an improvement of more than 10 dB—hearing improvement group. Fourteen patients showed no changes in the hearing levels, whereas three showed more than 10 dB decrease in hearing (Table 2). There was no difference in hearing level during the pre-GM periods between the hearing loss/no changes group and the hearing improvement group (Table 2). Moreover, among seven patients who had dominant −SP before GM, no one became negative for dominant −SP in the hearing loss/no changes group. In contrast, four of the eight patients became negative for dominant −SP in the hearing improvement group. This was a significant change as compared with the hearing loss/no changes group (Table 2, $p = 0.012$). Plasma AVP level before GM was lower in the hearing improvement group than that in the hearing loss/no changes group. (Table 2, $p = 0.0242$).

DISCUSSION

Vertigo Control

In this prospective study, five patients needed additional GM injections or vestibular neurectomy for vertigo control (Group I), although 23 patients were cured by three GM injections (Group II). Except for one case that underwent vestibular neurectomy, 27 of 28 patients eventually had their vertigo controlled by GM treatment. However, there were differences in several parameters between Groups I and II, which would account for the different effective mechanisms involved in the GM treatments.

There was no difference in the number of vertigo spells per month before intratympanic GM between Groups I and II, indicating that the frequency of the vertigo is not a key factor in the vertigo control after GM injections (Fig. 1). In contrast, hearing thresholds were higher in Group I than in Group II before GM injections (Fig. 2), suggesting that effects of GM injections may be more pronounced in patients with milder preinjection hearing loss.

An increase in CP% (Fig. 3) and an induction of post-HSN (Table 1) were observed after intratympanic GM only in Group II but not in Group I. Both results indicate that the induction of the vestibular damage in the injected ear is essential to the control of vertigo. Poor control of vertigo in Group I may be caused by the insufficient damage to the vestibular periphery perhaps because of drug delivery problems. Indeed, of the five Group I patients, one had a chronic otitis media, which would have made the GM perfusion through the round window less effective. Additional intratympanic GM to the Group I patients induced a progression of CP% and an appearance of post-HSN, resulting in a control of vertigo spells. Although previous studies demonstrated a variety of changes in caloric responses after GM treatments, there are limited data describing the relationships between the vestibular function and treatment outcome, which is a controversial issue; no correlation has been reported (11,12), whereas some other studies revealed correlation between vertigo control and vestibular ablation (13,14). Moreover, it has been hypothesized that intratympanic GM would even induce the recovery of the vestibular function by inhibiting or reducing endolymphatic hydrops via damage to the secretory function of vestibular dark cells (15,16), although a recent report (17) contradicts this theory. However, we suggest that intratympanic GM injections damage vestibular hair cells and thereby block the neurotransmission between hair cells and the vestibular nerve, resulting in a decrease of vertigo spells.

Hearing Changes

Damage to the cochlear function is the major concern of the intratympanic GM. In the present study, only 3 of 28 patients showed a decrease of more than 10 dB in hearing levels, suggesting that our protocol, one GM injection per day for three consecutive days, is a relatively safe procedure for cochlear damage.

In contrast, 11 of the 28 patients showed an improvement of more than 10 dB in hearing levels (Table 2). Whether this recovery of cochlear function is a direct effect of GM remains unclear. If so, simultaneous recovery of the vestibular function would be expected. However, CP% was increased after GM, and the vestibular periphery was damaged even in patients with hearing improvement (Fig. 3C), suggesting that the hearing improvement after intratympanic GM may be an indirect rather than a direct effect of GM on the cochlea. We, therefore, assume that hearing improvement only in Group II but not in Group I (Fig. 2) was a consequence of a good vertigo control rather than a direct effect of GM on the inner ear. The hearing results of our protocol seem better as compared with those of the most previous reports (18). However, given that this effect may be a secondary one, we do not recommend GM injections as a tool for hearing improvement in Ménière's patients.

As shown in Table 2, dominant −SP never disappeared in patients whose hearing was not improved; however, four of eight patients became negative for dominant −SP in the hearing improvement group. We assume that this recovery from endolymphatic hydrops is also